Journal of Medicinal Chemistry

Article

Cite This: J. Med. Chem. 2018, 61, 9952−9965

pubs.acs.org/jmc

Discovery and Structure−Activity-Relationship Study of *N*-Alkyl-5-hydroxypyrimidinone Carboxamides as Novel Antitubercular Agents Targeting Decaprenylphosphoryl-β-D-ribose 2′-Oxidase

Sangmi Oh,[†] Yumi Park,[†] Curtis A. Engelhart,[‡] Joshua B. Wallach,[‡] Dirk Schnappinger,[‡] Kriti Arora,[†] Michelle Manikkam,[†] Brian Gac,[†] Hongwu Wang,[§] Nicholas Murgolo,[§] David B. Olsen,[§] Michael Goodwin,[†] Michelle Sutphin,[†] Danielle M. Weiner,[†] Laura E. Via,[†,∥] Helena I. M. Boshoff,[†] and Clifton E. Barry, III*[,†,∥]

[†]Tuberculosis Research Section, Laboratory of Clinical Immunology and Microbiology, National Institute of Allergy and Infectious Diseases, National Institutes of Health, Bethesda, Maryland 20892, United States

[‡]Department of Microbiology and Immunology, Weill Cornell Medical College, New York, New York 10021, United States

[§]Discovery Research, Merck & Company, Inc., 770 Sumneytown Pike, West Point, Pennsylvania 19486, United States

[∥]Institute for Infectious Disease and Molecular Medicine, University of Cape Town, Cape Town 7935, South Africa

Supporting Information

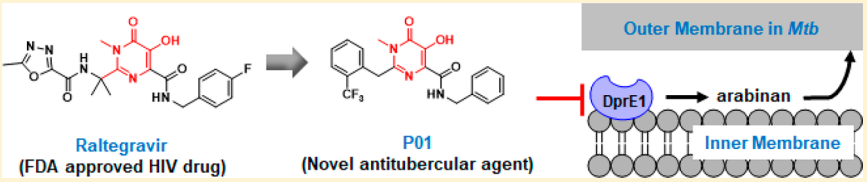

ABSTRACT: Magnesium plays an important role in infection with *Mycobacterium tuberculosis* (*Mtb*) as a signal of the extracellular environment, as a cofactor for many enzymes, and as a structural element in important macromolecules. Raltegravir, an antiretroviral drug that inhibits HIV-1 integrase is known to derive its potency from selective sequestration of active-site magnesium ions in addition to binding to a hydrophobic pocket. In order to determine if essential *Mtb*-related phosphoryl transfers could be disrupted in a similar manner, a directed screen of known molecules with integrase inhibitor-like pharmacophores (*N*-alkyl-5-hydroxypyrimidinone carboxamides) was performed. Initial hits afforded compounds with low-micromolar potency against *Mtb*, acceptable cytotoxicity and PK characteristics, and robust SAR. Elucidation of the target of these compounds revealed that they lacked magnesium dependence and instead disappointingly inhibited a known promiscuous target in *Mtb*, decaprenylphosphoryl-β-D-ribose 2′-oxidase (DprE1, Rv3790).

INTRODUCTION

Tuberculosis (TB) remains a global threat despite more than a century of research on its etiologic agent, *Mycobacterium tuberculosis* (*Mtb*). According to the WHO, in 2016, 10.4 million people were newly infected by TB, and 1.3 million people died from this disease.[1] Treatment of drug-sensitive TB requires at least 6 months of chemotherapy using drugs that were introduced into the market several decades ago, whereas treatment of multidrug- and extensively drug-resistant TB incorporate more drugs into an already complex treatment regimen, thereby increasing the duration of chemotherapy up to 24 months. The financial burden of TB chemotherapy also increases dramatically for the diagnosis and treatment of drug-resistant TB and was estimated to have incurred a global cost of US$2.0 billion in 2017, severely straining resource-constrained TB-control programs.[1] New agents that inhibit novel targets are one strategy to strengthen the repertoire of candidates in the drug-development pipeline that may lead to simplified chemotherapy for drug-sensitive TB and better options for drug-resistant-TB therapy.[2,3]

Mg^{2+} is important in all bacteria, serving, for example, as an important counterion for ATP in numerous enzyme reactions, enabling the formation of the tertiary structure of the bacterial ribosome, and contributing to the stability of lipid bilayers in cell envelopes.[4−6] In *Mtb*, two systems have been implicated in Mg^{2+} homeostasis, PhoPR and MgtC, which directly or indirectly exert broad control over various aspects of mycobacterial metabolism. The PhoP system, which in Enterobacteriaceae regulates Mg^{2+} levels and controls virulence,[7] plays a role in controlling several families of virulence-associated methyl-branched fatty acid containing acyl trehaloses that are unique to the pathogenic mycobacterial species.[8] PhoP-deficient mutants cannot grow in low concentrations of Mg^{2+}, do not replicate in macrophages, and fail to establish or

Received: June 4, 2018
Published: October 10, 2018

DOI: 10.1021/acs.jmedchem.8b00883
J. Med. Chem. 2018, 61, 9952−9965

maintain infections in mouse lungs.[9] MgtC is a Mg^{2+}-responsive virulence factor thought to function by interacting with the F_1F_0 ATP synthase,[10] which was discovered in *Mtb* by homology to a well-studied analogue in *Salmonella*.[11] Like mutants lacking PhoP, *mgtC* mutants are impaired for growth in low concentrations of Mg^{2+} in a mildly acidic environment, do not replicate in macrophages, and fail to grow in murine lungs and spleens.[12] The reliance by *Mtb* on Mg^{2+} as both a signal and a cofactor spurred our interest in potential therapeutic strategies that impact these systems.

Target-based approaches to TB drug discovery have not afforded any of the drugs in the preclinical or clinical development pipeline. Whole-cell screening has been most successful in identifying hits of interest with subsequent efforts dedicated to lead development and unraveling mechanisms of action.[13] However, the hit rates of commercially available small-molecule libraries are often quite low, and the hits often possess low structural diversity and poor physicochemical properties.[14] In contrast, small-molecule collections based on privileged scaffolds offer the potential of libraries encompassing attractive physicochemical properties and containing core scaffolds known to target a diversity of cellular targets, thereby increasing the likelihood of acceptable hit rates with compounds that inhibit specific targets. Privileged structures are defined as chemical scaffolds that could afford potent and selective small-molecule regulators for different kinds of biomolecules.[14−16] Therefore, privileged structures typically display favorable druglike properties, resulting in more high-quality leads. The dihydroxypyrimidine or pyrimidinedione scaffold is considered a privileged scaffold found in many biologically active molecules. The broad-ranging pharmacological roles generated by the pyrimidinedione moiety include antiviral agents,[17,18] antibacterial and antifungal agents,[19−21] and kinase inhibitors.[22] Among them, Raltegravir, a Mg^{2+}-dependent integrase inhibitor developed by MSD, is a good example of an antiretroviral drug with a pyrimidinedione scaffold.[23−25] In an effort to select hits that involve Mg^{2+}-dependent processes, we were interested in exploring the activity of the Mg^{2+}-chelating pyrimidinediones.

In this work, a novel series of *N*-alkyl-5-hydroxypyrimidinone carboxamides with antibacterial activity against *Mtb* is reported. The initial hit compound, **P01**, was derived from high-throughput screening of a library provided by St. Jude Children's Research Hospital that contained diverse pyrimidinedione derivatives as a privileged substructure.[26] Preliminary structure−activity-relationship (SAR) studies of the hit against *Mtb* were explored, as well as preliminary characterization of its biochemical target, decaprenylphosphoryl-β-D-ribose 2′-oxidase (DprE1), identified by resistance selection followed by whole-genome sequencing.

RESULTS AND DISCUSSION

High-Throughput Screening of Pyrimidinedione Library. The pyrimidinedione scaffold is a core for a diverse range of compounds inhibiting a multitude of potentially Mg^{2+}-dependent targets on the basis of the cation dependence of Raltegravir binding to its target. As a result, we decided to screen under a growth condition that supported robust in vitro growth with modest Mg^{2+} concentrations to exclude compounds that exert toxicity simply by cation chelation. Thus, a pyrimidinedione library containing 6207 compounds was screened for inhibition of growth of *Mtb* in a single-point assay at 10 μM final concentration. In medium containing glucose/glycerol/Tween 80 as the carbon sources with a final Mg^{2+} concentration of 0.2 mM, 38 hits (hit rate of 0.6%) giving >50% growth inhibition over a 3 day incubation period were generated. These hits were further validated in dose titrations by full MIC determination. To observe any Mg^{2+}-dependence of the hits and to diminish the effects of protein binding, these assays were performed in minimal medium (GAST) containing either 0.06, 6, or 60 mM $MgCl_2$, representing the lowest concentration that still supports *Mtb* growth, the standard in vitro Mg^{2+} concentration, and the 10-fold higher in vitro Mg^{2+} concentration, respectively. Three compounds having similar scaffolds exerted submicromolar inhibition of *Mtb* growth for up to 19 days of incubation with little evidence of rescue in response to increasing extracellular Mg^{2+} concentrations. One of these (**P01**) was chosen for further follow-up after consideration of structural aspects. As shown in Figure 1, **P01** is a *N*-methyl-5-hydroxypyrimidinone

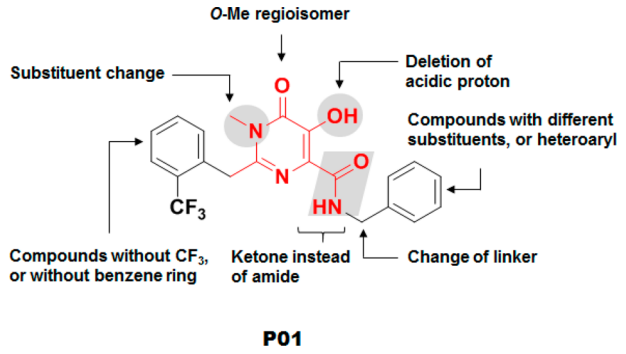

Figure 1. Hit compound **P01** and its derivatization for the SAR study.

derivative conjugated with a substituted benzyl group on the left-hand side and a benzyl-substituted carboxamide moiety on the right-hand side. Preliminary biological profiling of resynthesized **P01** was performed to verify that the compound was active independent of carbon source and to determine whether the compound inhibited targets in mycolyl-arabinogalactan biosynthesis or induced DNA damage as previously described.[27] The effect of the compound on the inhibition of respiratory metabolism was also assessed using the *cyd*::*aph* strain.[28] The compound was found to be active under all replicating conditions with decreased activity in the slow-growth assay wherein *Mtb* is subjected to the suboptimal environment of acidic pH and nitrosative stress (Table 1). The cell-wall-reporter assay hinted that the compound might affect a target in cell-wall biosynthesis, as evidenced by the upregulation of the *iniBAC* promoter.

Synthesis of Derivatives and Their Structure−Activity Relationship. To understand the structural aspects of the initial hit that were critical for antitubercular activity, a series of pyrimidinedione derivatives, modified in each moiety of the original structure, were designed and prepared. The general synthesis of *N*-alkyl-5-hydroxypyrimidinone carboxamides **P01**−**P13** is described in Scheme 1. For the formation of the dihydroxypyrimidine ring, previously reported procedures starting from nitrile derivatives (**1**) were used.[18,29−31] Briefly, amidoximes **2** were prepared from nitriles **1** after reactions with salt-free hydroxylamine. Next, Michael-type addition reaction of **2** with dimethyl acetylenedicarboxylate followed by intramolecular cyclization generated dihydroxypyrimidine intermediates **4**−**6**. After benzoyl protection of the 5-hydroxyl

DOI: 10.1021/acs.jmedchem.8b00883
J. Med. Chem. 2018, 61, 9952−9965

Table 1. Biological Aspects of Hit Compound P01

	MIC (μM)[a]						reporter-gene assay	
hit	7H9/ADC[b]	GAST	GBSA or DBSA[c]	nitrite/butyrate[d]	Chol[e]	CydKO[f]	cell wall[g]	DNA damage[h]
P01	4.7 ± 1.5	0.4 ± 0.2	3.1	12.5	1.6	6.2	positive	no induction

[a]MIC of compound against *Mtb* strain H37Rv in the different media. [b]Middlebrook 7H9/BSA containing glucose/glycerol/Tween 80. [c]Middlebrook 7H9/BSA/Tyloxapol with glucose (GBSA) or dipalmitoylphosphatidylcholine (DBSA) as the carbon source. [d]Middlebrook 7H9/BSA/Tyloxapol/butyrate/0.1 mM sodium nitrite, pH 6.0. [e]Middlebrook 7H9/BSA/Tyloxapol/cholesterol. [f]Middlebrook 7H9/ADC with *cydC*::*aph*. [g]Induction of the cell-wall responsive *iniBAC* promoter as measured using the piniB-LUX reporter strain. [h]Induction of the DNA-damage responsive *recA* and *radA* reporters using the precA-LUX and pradA-LUX reporter strains.

Scheme 1. General Synthetic Scheme of *N*-Alkyl-5-hydroxypyrimidinone Carboxamide Derivatives[a]

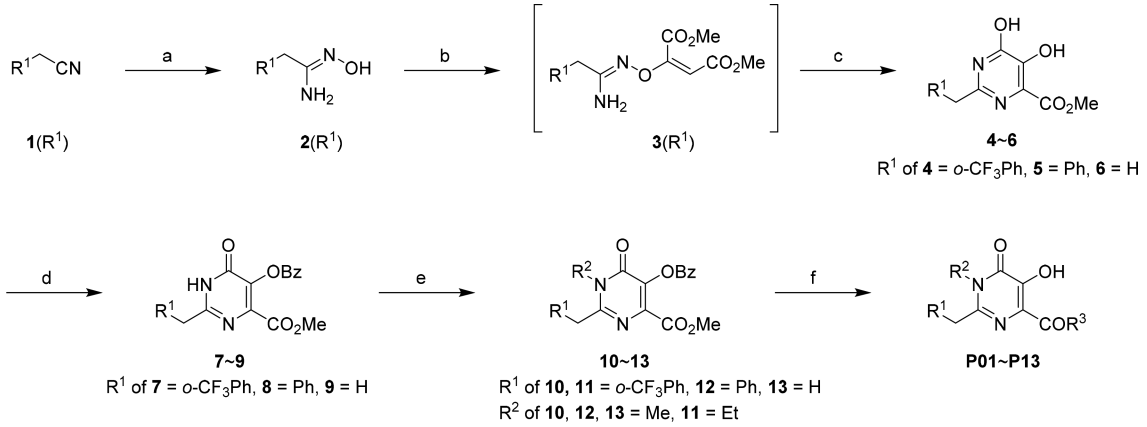

[a]Reagents and conditions: (a) $HONH_2$·HCl, KOH, MeOH, reflux, 6 h; (b) dimethyl acetylenedicarboxylate, MeOH, rt, overnight; (c) xylene, reflux, overnight; (d) BzCl, pyridine, rt, overnight; (e) R^2I, Cs_2CO_3, THF; (f) amine or aniline (R^3–H), MeOH, reflux, overnight.

Scheme 2. Synthesis of Pyrimidinedione Derivatives P14–P17[a]

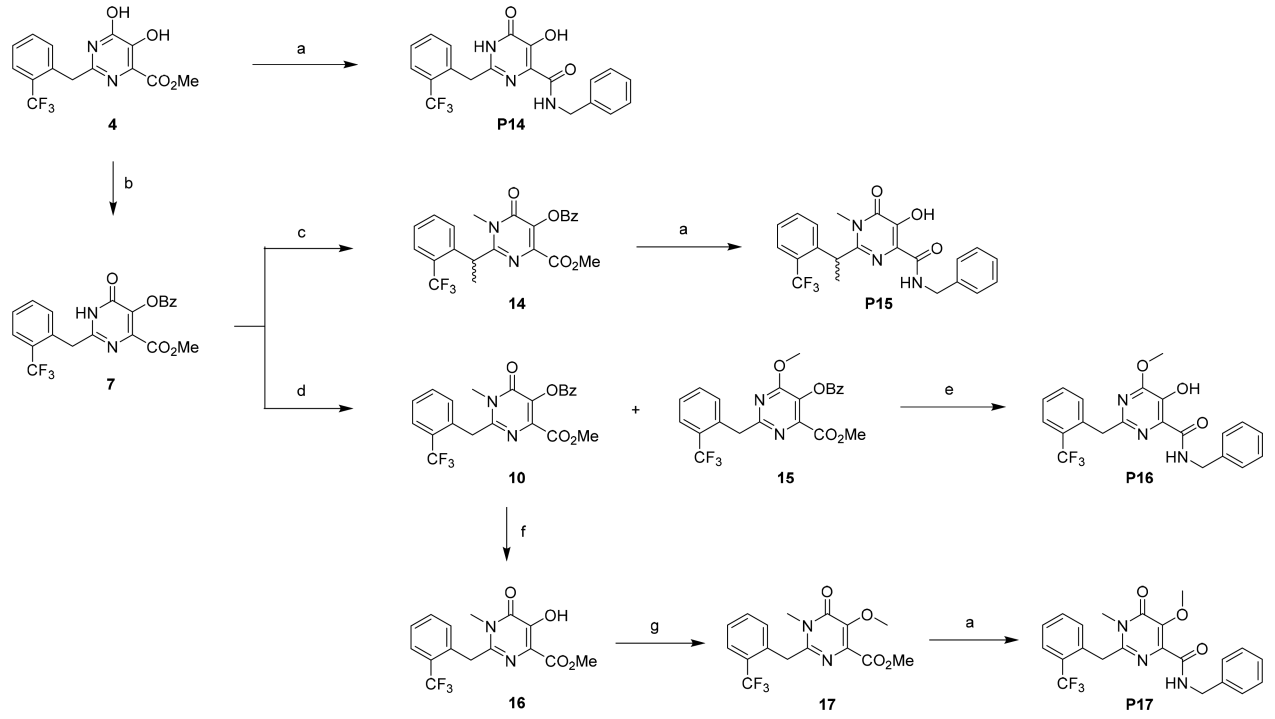

[a]Reagents and conditions: (a) benzylamine (3 equiv), MeOH, reflux, overnight; (b) BzCl, pyridine, rt, overnight; (c) MeI (5 equiv), Cs_2CO_3 (3 equiv), THF, 40 °C, overnight; (d) MeI (3 equiv), K_2CO_3 (2 equiv), DMF, rt, 4 h; (e) benzylamine (2.2 equiv), reflux, 30 min; (f) *N*-benzylmethylamine, MeOH, reflux, 3 h; (g) $TMSCHN_2$, $CHCl_3$/MeOH, rt, overnight.

group, alkylation on the N3 position mediated by Cs_2CO_3 followed by a thermal amidation reaction produced the desired products, **P01–P13**.

To validate the importance of the alkyl group at the N3 position, **P14**, without the methyl substituent, was synthesized by direct thermal amidation from intermediate **4** (Scheme 2).

DOI: 10.1021/acs.jmedchem.8b00883
J. Med. Chem. 2018, 61, 9952–9965

During N3-methylation in the presence of MeI and Cs_2CO_3, the addition of excess amounts of reagents, higher temperature, and a longer reaction time gave rise to the formation of overmethylated compound **14**, which was the precursor of **P15**. In addition, the *O*-Me regioisomer, **15**, was also produced as a byproduct during methylation. Structurally, the *O*-Me group in the pyrimidine ring was easily substituted by benzylamine during the thermal amidation reaction, allowing the reaction time for the synthesis of **P16** to be shortened to avoid oversubstitution by benzylamines. To incorporate another methyl group in the acidic 5-hydroxyl position, **16**, generated from **10** by debenzoylation, was methylated by trimethylsilyldiazomethane to afford the methylated compound, **P17**.[17]

The synthesis of **P18**, which has the ketone functionality at the position of C6 normally occupied by the amide, is shown in Scheme 3. The 5-hydroxyl group in **16** was benzylated, and

Scheme 3. Synthesis of Pyrimidinedione Derivative P18[a]

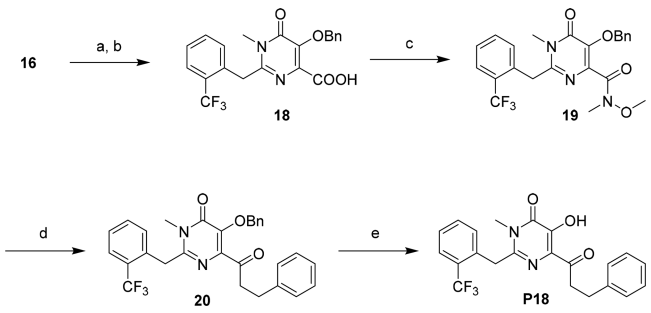

[a]Reagents and conditions: (a) BnBr, KI, K_2CO_3, DMF, 80 °C, overnight; (b) NaOH, MeOH/H_2O, rt, 3 h; (c) CDI, CH_2Cl_2, rt, 1 h, and then *N*,*O*-dimethylhydroxylamine·HCl, TEA, rt, overnight; (d) generation of the Grignard reagent using (2-chloroethyl) benzene, Mg, and 1,2-dibromethane in THF, and then rt, 2 h; (e) 10% Pd/C, H_2, MeOH/THF, rt, 1 h.

subsequent basic hydrolysis afforded **18**.[32] The carboxylic moiety of **18** was transformed into Weinreb amide **19**, which underwent selective monoaddition of Grignard reagent produced by (2-chloroethyl)benzene to generate the corresponding ketone, **20**, with **P18** obtained after debenzylation.[33]

All final compounds (**P01**−**P18**) were fully characterized by LC-MS and ^{1}H and ^{13}C NMR. In addition, HRMS and melting-point analyses were performed for some active compounds. Antitubercular activities of synthetic compounds in two different media and their cytotoxicity against HepG2 cells are summarized in Table 2.

Initial SAR studies around the hit compound, **P01**, focused on identifying key moieties or functionalities that play important roles in antitubercular activity. This focused library of 18 compounds (**P01**−**P18**), constructed for preliminary SAR, guided the next steps for hit-to-lead modification, despite its small size. Compounds **P02**−**P03** and **P15** were synthesized to evaluate the left-hand-side modification of R^1. The benzene ring was necessary for antitubercular activity, as seen by complete loss of potency in the absence of this moiety (**P03**), with the *o*-CF_3 substitution (**P01**) further improving potency. A methyl substitution in the benzylic position was detrimental for activity, as seen by the 5-fold increase in the MIC of **P15** compared with that of the initial hit, **P01**.

To assess the importance of the methyl group in the N3 position, two compounds, including **P04** with an ethyl group and **P14** without an alkyl substituent, were synthesized. Replacement of the methyl (**P01**) by the ethyl group (**P04**) showed good potency with improved MICs (2.3 μM in 7H9/ADC and 0.4 μM in GAST), but deletion of the methyl at this position (**P14**) was not tolerated. Not surprisingly, the *O*-Me regioisomer (**P16**) was inactive against *Mtb*. Methyl protection of the acidic 5-hydroxyl group also resulted in loss of antitubercular activity. These results demonstrate that the *N*-alkyl-5-hydroxypyrimidinone core was critical for retaining potency against this pathogen.

The compounds **P05**−**P13** and **P18** were synthesized to determine SAR of the right-hand side R^3 position. As shown in Table 2, the benzyl group at the R^3 position was important for antitubercular activity because its replacement by a phenyl group (**P05**) reduced potency around 4-fold over **P01**, and the saturated cyclohexyl methyl group (**P06**) was also less potent with likely increased protein binding, as evidenced by its lack of activity in BSA-containing Middlebrook 7H9-based medium. Replacement of the phenyl with certain heteroaryl groups, such as the 2-picolyl moiety (**P07**), was tolerated at the R^3 position, but its regioisomer, 3-picolyl (**P08**), showed a decrease in activity. Initial investigations into substituent effects on the benzene ring revealed that *o*-F (**P09**) was tolerated with a potency similar to that of **P01**, and it was >4-fold more potent than its regioisomer, **P10**, with *p*-F. Interestingly, the compound with the benzodioxole moiety replacing the benzene ring (**P11**) was completely inactive against *Mtb*, indicating that substituent effects in the benzene ring were important for the antitubercular activity of this scaffold. Conformational restriction of amide linkage by *N*-methylation (**P12**) as well as methylation of the benzylic position (**P13**) resulted in loss of activity. In addition, the amide functionality was important because **P18**, with a ketone replacing the amide at R^3, was inactive. None of the derivatives were cytotoxic against HepG2 cells and additionally did not exert overt mitochondrial toxicity as seen by lack of cytotoxicity during growth of these cells on galactose as a carbon source (Table 2).

The pharmacokinetic (PK) parameters of C57BL/6 mice administered a single 10 mg/kg oral suspension of **P01** indicated absorption was fairly low (C_{max} 0.25 μg/mL, AUC of 1.06 μg·h/mL), but the half-life of 4 h and V_d of 33.7 L/kg were acceptable (Table 3). Even though PK parameters are encouraging as a starting point of in-depth medicinal chemistry, efficacy studies in mice were not pursued with this hit compound because PK modeling suggested a much higher dose would be needed to achieve an average plasma concentration above the MIC of **P01** (~1.9 μg/mL in 7H9/ADC) because of the high murine metabolic rate.

Activity Validation in Vitro and ex Vivo and Target-Protein Identification using Whole-Genome Sequencing. The hit compound, **P01**, was bactericidal to actively replicating *Mtb* in vitro, with a 1−2 logarithmic reduction in colony-forming units observed over 7 days with weak dose-dependence across a wide range of concentrations (Figure 2A), but it lacked bactericidal activity against anaerobic non-replicating *Mtb* cells generated in the Wayne model of hypoxic adaptation (Figure 2B).[34] The parental hit compound (**P01**) and three of its in vitro active analogues (**P04**, **P07**, and **P09**) were also active against *Mtb* replication in J774 murine macrophages, indicating that the compound retained bactericidal activity under these conditions and was also able to reach the pathogen in its phagosomal niche (Figure 2C).

DOI: 10.1021/acs.jmedchem.8b00883
J. Med. Chem. 2018, 61, 9952−9965

Table 2. Structural Aspects and Antitubercular Activities of Compounds P01−P18

Compound	Chemical Structure			MIC (μM)		Cytotoxicity (IC_{50}, μM)	
	R^1	R^2	R^3	7H9/ADC[a]	GAST[b]	Glucose[c]	Galactose[d]
P01	*o*-CF_3Ph	Me		4.7	0.59	>100	>100
P02	Ph	Me		9.4	3.1	>100	>100
P03	H	Me		>100	>100	>100	>100
P04	*o*-CF_3Ph	Et		2.3	0.39	>100	>100
P05	*o*-CF_3Ph	Me		18.8	1.6	>100	>100
P06	*o*-CF_3Ph	Me		>100	12.5	>100	>100
P07	*o*-CF_3Ph	Me		3.1	1.2	>100	>100
P08	*o*-CF_3Ph	Me		18.8	4.7	>100	>100
P09	*o*-CF_3Ph	Me		4.7	0.59	>100	>100
P10	*o*-CF_3Ph	Me	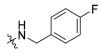	18.8	2.3	>100	>100
P11	*o*-CF_3Ph	Me	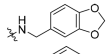	>100	37.5	>100	>100
P12	*o*-CF_3Ph	Me		>100	>100	>100	>100
P13	*o*-CF_3Ph	Me		>100	>100	>100	>100
P14	*o*-CF_3Ph	H		>100	>100	>100	>100
P15	N/A[e] (see Scheme 2)			18.3	3.1	>100	>100
P16	N/A (see Scheme 2)			>100	37.5	>100	>100
P17	N/A (see Scheme 2)			>100	>100	>100	>100
P18	N/A (see Scheme 3)			100	12.5	>100	>100

[a]MIC of compound tested against *Mtb* H37Rv in Middlebrook 7H9/ADC. [b]MIC of compound tested against *Mtb* H37Rv in GAST. See the Experimental Section. [c]Cytotoxicity of compound tested against HepG2 cells in DMEM/10% FBS supplemented with glucose. [d]Cytotoxicity of compound tested against HepG2 cells in DMEM/10% FBS with galactose. [e]Not available. Chemical structures described in Schemes 2 and 3.

Table 3. Oral Exposure of P01 in Mice after a Single Dose

PK property[a]	unit	**P01**
C_{max}	μg/mL	0.25
T_{max}	h	1.0
$T_{1/2}$	h	4.1
AUC	μg·h/mL	1.06
V_d	L/kg	33.7
CL	μg/h	9.48

[a]Pharmacokinetic parameters of **P01** in C57Bl/6 mice dosed orally with 10 mg/kg.

To identify the putative target of **P01**, resistant mutants were generated by plating of *Mtb* on solid-medium plates containing 1×, 2×, 5×, and 10× MIC concentrations of the compound, with a mutation frequency of 7×10^{-9} obtained at 10× MIC. Twenty-four **P01**-resistant mutants were tested for their level of resistance by MIC determination against **P01**, and all were found to be more than 10-fold resistant compared with the parental strain. Four of these resistant strains were submitted for whole-genome sequencing. All four were found to contain the same Y314H mutation in decaprenylphosphoryl-β-D-ribose 2′-oxidase (DprE1, Rv3790). DprE1 together with DprE2 catalyzes the epimerization of decaprenylphosphoryl ribose (DPR) to decaprenylphosphoryl arabinose (DPA) in the synthesis of cell-wall-linked arabinan.[35] DprE1 has already been established as a highly vulnerable target in mycobacterial cell-wall biosynthesis as seen by the high number of chemically diverse scaffolds that inhibit this essential target, leading to cellular-growth inhibition both in vitro and in vivo.[36,37] The high frequency of hits against this target is likely also driven by its extra-cytoplasmic localization in the periplasmic face of the plasma membrane. The validity of inhibiting this target as a viable strategy in TB chemotherapy will be tested in the ongoing clinical trial of a benzothiazinone compound (PBTZ169).[38] To further confirm that the *N*-alkyl-5-hydroxypyrimidinone carboxamides inhibited DprE1, we tested the vulnerability of a panel of diverse *dprE1* mutants to **P01**. Strains with the Y314C and P116S substitutions but not the N346S mutation in DprE1 were found to be cross-resistant to **P01** (Table 4). Y314C has previously been observed to confer resistance to the DprE1 inhibitor TCA1[39] but not to the benzothiazinone scaffold.[40]

Target Validation using a Regulated Expression of the *dprE1*−*dprE2* Locus. The on-target activity of the *N*-alkyl-5-hydroxypyrimidinone carboxamides was further con-

DOI: 10.1021/acs.jmedchem.8b00883
J. Med. Chem. 2018, 61, 9952−9965

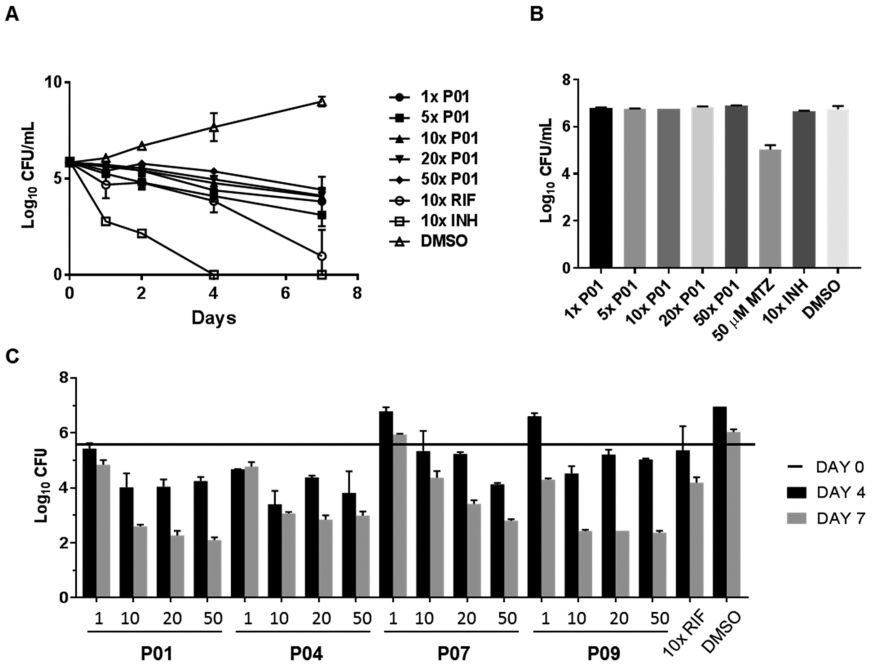

Figure 2. Activity of the hydroxypyrimidinone analogues in vitro and ex vivo. (A) Kill kinetics of **P01** at 1−50-fold MIC under replicating condition for 7 days. (B) **P01** lacking anaerobic bactericidal activity over 7 days of exposure, indicated at fold concentrations of the aerobic MIC. (C) Intracellular killing assay of hydroxypyrimidinone analogues in murine macrophage J774. Infected cells were treated at 1−50-fold MIC of analogues for 4 or 7 days, and then colonies were enumerated.

Table 4. Different Mutations in DprE1 Conferring Different Levels of Resistance to P01

DprE1 mutation	MIC (μM)	fold change
wild type	3.13	—
Y314H	>50	>16
Y314C	25	8
N364S[a]	2.34	0.75
P116S[a]	18.8	6

[a]Mutants raised against an undisclosed DprE1 inhibitor.

firmed using a strain in which the level of the DprE1−DprE2 epimerase complex was transcriptionally regulated by the tetracycline repressor, TetR. In this strain, *dprE1−dprE2* transcription is dependent on the presence of tetracycline. Removal of tetracycline results in repression of *dprE1−dprE2* and a concomitant increase in susceptibility to known DprE1 inhibitors, such as TCA1[39] and the benzothiazinone BTZ043[41] (Figure 3A,B), whereas ethambutol, which inhibits the downstream arabinosyltransferases, showed equipotent efficacy during *dprE1−dprE2* repression (Figure 3C). As expected, active compounds **P01** and **P04** exerted more growth inhibition of the mycobacterial cells during *dprE1−dprE2*-transcriptional repression (Figure 3D,E), whereas the inactive homologue **P13** did not result in growth inhibition of this regulated mutant (Figure 3F). The higher resistance of the tetracycline-regulated cells during treatment with TCA1, **P01**, and **P04** is likely driven by higher basal levels of protein of one or both of the DprE subunits. The clear shift in susceptibility during regulated expression of the subunits of this epimerase complex establishes the on-target activity of the *N*-alkyl-5-hydroxypyrimidinone carboxamides in whole cells.

Molecular-Docking Study of *N*-Alkyl-5-hydroxypyrimidinone Carboxamides in DprE1. Molecular modeling was used to understand the potential interactions of synthetic analogues with DprE1. Figure 4A shows the model of **P01** in the binding site of DprE1. An extensive hydrogen-bond (HB) network was formed between **P01** and the polar residues lining the interior of the binding site. The carbonyl oxygen atom of the pyrimidinone core formed an HB with the side-chain amino group of residue N385. The 5-hydroxyl group, with a pK_a of 4.5 as calculated by ACD Laboratories pK_a method,[42] was deprotonated, and the negatively charged oxygen atom formed HBs with both the H132 and Q336 side chains. Methylation of this oxygen atom as in **P17** disrupted the HBs, hence rendering the compound inactive. The exocyclic amide oxygen on the right-hand side formed an HB with the K418 side chain. The amide −NH group, on the other hand, formed an intramolecular HB with one nitrogen atom of the pyrimidinone core, stabilizing the ligand-bound conformation. Methylation of this group, as in **P12**, abolished this intramolecular HB, and the size of the methyl group forced the amide to rotate out of the plane of the pyrimidinone core, leading to the inactivity of **P12**. Replacing the amide − NH group with a methylene, as in **P18**, had a similar impact that reduced its binding affinity. Furthermore, the methyl group in the N3 position made hydrophobic contact with the side-chain carbon atoms of K367; demethylation here, as in **P16**, was likely the reason for its reduced activity.

Hydrophobic interactions with the DprE1 active site contributed substantially to the ligand-binding affinity. The trifluoromethyl group on the phenyl ring of the left-hand side made hydrophobic contacts with the side chain of Y314, whereas the phenyl ring itself engaged in hydrophobic interactions with the side chain of V365 at the bottom of the binding site. Deleting the *o*-CF_3 group lowered the binding affinity several-fold, as shown for **P02**, whereas removing the whole *o*-CF_3Ph moiety, as in **P03**, made the compound completely inactive. The phenyl ring on the right-hand side made a π−cation interaction with the R325 side chain.

DOI: 10.1021/acs.jmedchem.8b00883
J. Med. Chem. 2018, 61, 9952−9965

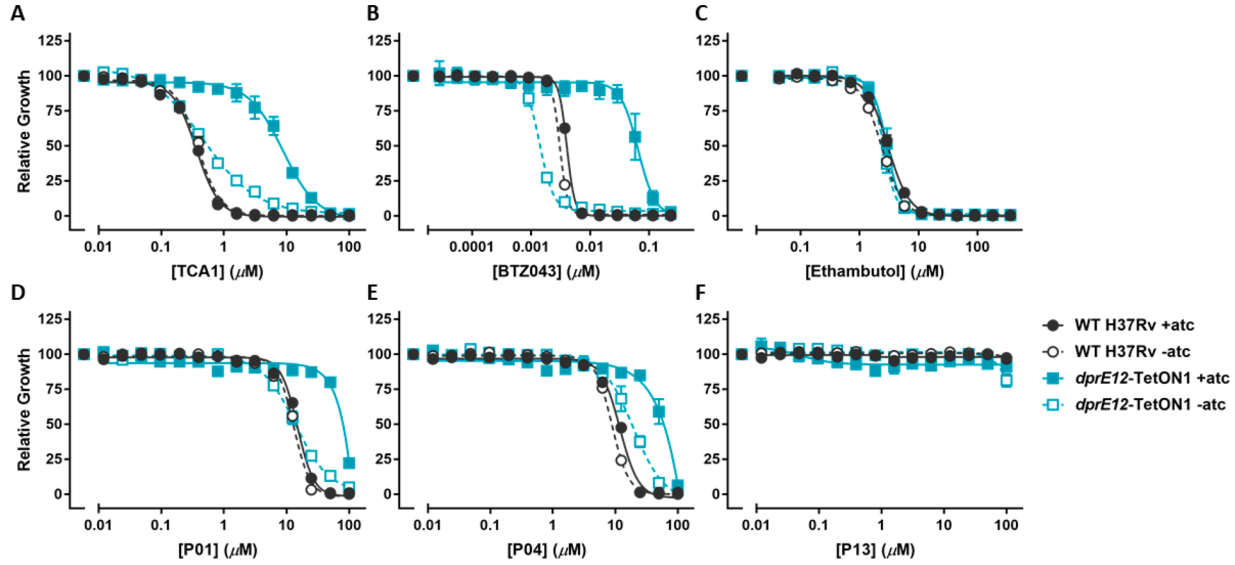

Figure 3. Hydroxypyrimidinone analogues targeting the DprE1−DprE2 enzymes in whole cells, as evidenced by increased vulnerability of a transcriptionally downregulated *dprE1−dprE2* mutant. Removal of anhydrotetracycline (atc) results in transcriptional repression of the *dprE1−dprE2* operon. Growth in the presence of the DprE1 inhibitor TCA1 (A); the covalent DprE1 inhibitor BTZ043 (B); the arabinosyltransferase inhibitor ethambutol (C); and compounds **P01** (D), **P04** (E), and **P13** (F) recorded relative to the DMSO-only control. Data are representative of two independent experiments.

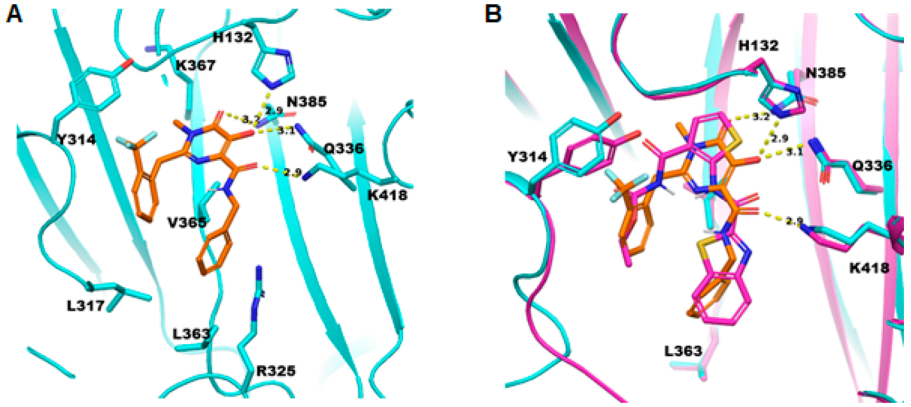

Figure 4. Molecular-docking study of **P01** in DprE1. (A) Docking model of **P01** in the binding site of *Mtb* DprE1 (PDB code: 4P8N). The protein structure is shown as a cyan-colored cartoon with the key residues involved the ligand binding displayed. The protein-side-chain carbon atoms are colored cyan, and the ligand (**P01**) carbon atoms are colored brown. Oxygen atoms are colored red, nitrogen atoms are colored blue, fluorine atoms are colored light cyan, and polar hydrogen atoms on the ligand are colored white. Hydrogen bonds between the ligand and the protein are depicted as yellow dashed lines. (B) Overlay of the **P01** model with the crystal structure of TCA1 in complex with DprE1 (PDB code: 4KW5). The carbon atoms of TCA1 are colored magenta. The TCA1-bound protein structure and the carbon atoms of the key residues are also colored magenta.

Replacing this group with a cyclohexyl moiety reduced this favorable interaction, and led to the low potency of **P06**. In addition, this phenyl group made hydrophobic contacts with the side chains of residues L317, L363, and V365. The size of the binding pocket around this phenyl group was not large enough to accommodate **P11**, hence its much lower potency.

The model of **P01** was compared with the crystal structure of a known DprE1 inhibitor, TCA1[39] (Figure 4B). The pyrimidinedione core of **P01** binds at the same subpocket as the thiophene core, both forming strong interactions with the H132 side chain. The amide carbonyl groups in both compounds formed hydrogen bonds with the side chain of K418. The distal benzyl group off the amide binds in the same hydrophobic region as the benzothiazole group of TCA1. Additionally, the other side of both molecules engages the Y314 side chain. This docking model and the similar interaction pattern with the DprE1 binding site in comparison with TCA1 provide further evidence that these compounds target *Mtb* DprE1.

CONCLUSIONS

In order to discover a novel candidate for the treatment of TB, we screened a pyrimidinedione library that contains this embedded privileged structure associated with magnesium-chelating properties and generated a new hit, *N*-alkyl-5-hydroxypyrimidinone carboxamide, **P01**. The SAR of **P01** was examined through the construction of 17 analogues, in which we comprehensively modified each moiety in the original scaffold. Even though the MICs of the active compounds were not dependent on Mg^{2+} concentration, they showed significant growth inhibition in each media without notable cytotoxicity.

DOI: 10.1021/acs.jmedchem.8b00883
J. Med. Chem. 2018, 61, 9952−9965

Through whole-genome sequencing of resistant mutants, we identified that this series targets DprE1, which is an essential enzyme for pathogen-specific cell-wall biogenesis. Several molecules that target DprE1 are in preclinical and clinical development,[43] but no drug targeting this enzyme has been approved for clinical use to date. The *N*-alkyl-5-hydroxypyrimidinone carboxamides represent a potentially viable alternative scaffold should current candidates fail to complete clinical development. These compounds have favorable solubility, toxicity, and PK properties that should provide adequate opportunity for lead optimization. Although it was disappointing to not identify scaffolds that potentiated Mg^{2+}-dependent processes in the cell, alternative screening procedures may still identify candidate molecules within this privileged core structure that do.

EXPERIMENTAL SECTION

Chemistry. ^{1}H and ^{13}C NMR spectra were recorded on a Varian Mercury-300 NMR Spectrometer, and chemical shifts were measured in parts per million relative to a specific solvent signal. Routine mass and purity analyses (LRMS) were performed on an HP Agilent LC-MS series 1100 system equipped with a reverse-phase column (Agilent Poroshell 120 EC-C18, 2.7 μm, 50 × 2.1 mm) and a photodiode-array detector coupled to an Agilent 1946 DSL quadrupole mass selective detector coupled to an Agilent 1946 DSL quadrupole mass selective detector using electrospray ionization (ESI). A gradient mobile phase consisting of acetonitrile/water with 0.1% formic acid and UV detection at 254 and 210 nm were used to confirm all final products (**P01**−**P18**) as being ≥95%. Melting points were measured on an Electrothermal 9100 apparatus. Accurate masses (HRMS) were obtained using a Waters LCT Premiere time-of-flight mass spectrometer. The instrument was operated in W-mode at a resolution of 10 000 in positive-ion mode. Ions were generated with Z-Spray electrospray ionization (ESI) with a capillary voltage of 3.4 kV. Accurate masses were determined using the internal-standard method. Most reagents used in the synthetic procedure were purchased from Sigma-Aldrich, Alfa Aesar, and TCI. The progress of the reaction was monitored using thin-layer chromatography (TLC; silica gel 60 F254 0.25 mm), and the products were visualized by UV light (254 and 365 nm). SiliaFlash P60 (40−60 μm) used in flash column chromatography was purchased from Silicycle Inc. Other solvents were purchased from commercial vendors and used without further purification unless otherwise mentioned.

Synthesis of P01−P17. *General Procedure for Pyrimidinedione Formation Starting from Substituted Acetonitrile.* Synthesis of pyrimidinedione intermediates **4**−**6** was performed using the previously reported procedure.[18,29−31]

*Methyl 5,6-Dihydroxy-2-(2-(trifluoromethyl)benzyl)pyrimidine-4-carboxylate (**4**).* Synthesis from the starting material, 2-(trifluoromethyl)phenylacetonitrile, was followed by a known procedure (overall 26%, brown solid): ^{1}H NMR (300 MHz, $(CD_3)_2SO$) δ 7.71 (d, J = 7.8 Hz, 1H), 7.61 (t, J = 7.6 Hz, 1H), 7.47 (t, J = 7.6 Hz, 1H), 7.32 (d, J = 7.5 Hz, 1H), 4.07 (s, 2H), 3.73 (s, 3H); ^{13}C NMR (75 MHz, $(CD_3)_2SO$) δ 168.3, 166.0, 159.3, 148.1, 145.2, 134.6, 132.6, 131.8, 127.4, 127.1, 126.0 (q), 122.6, 52.2, 36.4; LRMS (ESI) m/z 329 [M + H$^+$].

*Methyl 2-Benzyl-5,6-dihydroxypyrimidine-4-carboxylate (**5**).* Synthesis from the starting material, benzyl cyanide, was followed by a known procedure (overall 40%): ^{1}H NMR (300 MHz, $(CD_3)_2SO$) δ 10.24 (bs, 1H), 7.34−7.21 (m, 5H), 3.81 (s, 2H), 3.80 (s, 3H); ^{13}C NMR (75 MHz, $(CD_3)_2SO$) δ 166.1, 159.1, 149.3, 145.0136.6, 132.5, 128.6, 128.5, 126.7, 52.2, 40.7: LRMS (ESI) m/z 261 [M + H$^+$].

*Methyl 2-Ethyl-5,6-dihydroxypyrimidine-4-carboxylate (**6**).* Synthesis from the starting material, propionitrile, was followed by a known procedure (overall 11%): ^{1}H NMR (300 MHz, $(CD_3)_2SO$) δ 10.13 (bs, 1H), 3.80 (s, 3H), 2.47 (q, J = 7.5 Hz, 2H), 1.14 (t, J = 7.5 Hz, 3H); ^{13}C NMR (75 MHz, $(CD_3)_2SO$) δ 166.3, 159.1, 151.8, 144.8, 128.7, 52.1, 27.0, 11.5; LRMS (ESI) m/z 199 [M + H$^+$].

*General Procedure of Benzoylation in the 5-OH Group (**7**−**9**).* To a solution of **4** (1.0 equiv) in pyridine (0.5 M) was added benzoyl chloride (1.0 equiv) at rt. After being stirred overnight at rt, the reaction mixture was diluted with EtOAc and washed with 1 N HCl, saturated $NaHCO_3$, and brine. The organic layer was dried over Na_2SO_4 and evaporated in vacuo. The crude solid was suspended in EtOAc, filtered, and washed with Et_2O to obtain the desired product.

*Methyl 5-(Benzoyloxy)-6-oxo-2-(2-(trifluoromethyl)benzyl)-1,6-dihydropyrimidine-4-carboxylate (**7**).* Off-white solid (69%): R_f = 0.43 (EtOAc/hexane = 1/1); ^{1}H NMR (300 MHz, $CDCl_3$) δ 8.16 (d, J = 7.2 Hz, 2H), 7.66 (t, J = 7.2 Hz, 1H), 7.56−7.48 (m, 4H), 7.38−7.33 (m, 2H), 4.26 (s, 2H), 3.83 (s, 3H); ^{13}C NMR (75 MHz, $CDCl_3$) δ 163.5, 163.1, 159.2, 156.3, 143.4, 138.2, 134.2, 132.7, 131.9, 130.7, 129.1, 128.8, 128.3, 128.2, 126.7 (q), 125.9, 122.3, 53.4, 38.4; LRMS (ESI) m/z 433 [M + H$^+$].

*Methyl 5-(Benzoyloxy)-2-benzyl-6-oxo-1,6-dihydropyrimidine-4-carboxylate (**8**).* Off-white solid (72%): R_f = 0.29 (EtOAc/hexane = 1/1); ^{1}H NMR (300 MHz, $CDCl_3$) δ 8.24 (d, J = 8.4 Hz, 2H), 7.69 (t, J = 7.5 Hz, 1H), 7.56 (t, J = 7.6 Hz, 2H), 7.31−7.27 (m, 5H), 4.03 (s, 2H), 3.90 (2, 3H); ^{13}C NMR (75 MHz, $CDCl_3$) δ 163.5, 163.2, 160.2, 157.9, 143.9, 137.9, 134.3, 134.0, 130.7, 129.5, 129.2, 128.9, 128.3, 128.0, 53.4, 42.0; LRMS (ESI) m/z 365 [M + H$^+$].

*Methyl 5-(Benzoyloxy)-2-ethyl-6-oxo-1,6-dihydropyrimidine-4-carboxylate (**9**).* Off-white solid (55%): R_f = 0.19 (EtOAc/hexane = 1/1); ^{1}H NMR (300 MHz, $CDCl_3$) δ 8.19 (d, J = 8.4 Hz, 2H), 7.67 (t, J = 7.5 Hz, 1H), 7.53 (t, J = 7.5 Hz, 2H), 2.73 (q, J = 7.5 Hz, 2H), 1.29 (t, J = 7.5 Hz, 3H); ^{13}C NMR (75 MHz, $CDCl_3$) δ 163.7, 163.3, 160.8, 160.7, 144.2, 137.5, 134.2, 130.6, 128.8, 128.4, 53.4, 28.9, 11.6; LRMS (ESI) m/z 303 [M + H$^+$].

*General Procedure of Alkylation Mediated by Cs_2CO_3 (**10**−**13**).* To a solution of starting material (1.0 equiv) in anhydrous THF (0.2 M) were added Cs_2CO_3 (2.0 equiv) and alkyl iodide (2.5 equiv). The reaction mixture was stirred at rt for about 5 h in the case of methylation or stirred overnight at 40 °C in the case of ethylation. The reaction mixture was diluted with EtOAc and washed with 1 N HCl and brine. The organic layer was dried over Na_2SO_4 and evaporated in vacuo. The crude mixture was purified by flash column chromatography (EtOAc/hexane) to obtain the desired product.

*Methyl 5-(Benzoyloxy)-1-methyl-6-oxo-2-(2-(trifluoromethyl)-benzyl)-1,6-dihydropyrimidine-4-carboxylate (**10**).* Off-white solid (79%): R_f = 0.53 (EtOAc/hexane = 1/1); ^{1}H NMR (300 MHz, $CDCl_3$) δ 8.17 (d, J = 8.1 Hz, 2H), 7.70 (d, J = 7.8 Hz, 1H), 7.62 (t, J = 7.9 Hz, 1H), 7.48 (t, J = 7.7 Hz, 2H), 7.39 (t, J = 7.5 Hz, 1H), 7.07 (d, J = 7.2 Hz, 1H), 4.43 (s, 2H), 3.81 (s, 3H), 3.37 (s, 3H); ^{13}C NMR (75 MHz, $CDCl_3$) δ 163.6, 163.1, 158.6, 156.6, 140.5, 137.7, 134.1, 132.7, 132.6, 130.6, 128.9, 128.7, 128.4, 128.3, 128.0, 127.8, 126.7 (q), 126.1, 122.4, 53.1, 38.8, 31.9; LRMS (ESI) m/z 447 [M + H$^+$].

*Methyl 5-(Benzoyloxy)-1-ethyl-6-oxo-2-(2-(trifluoromethyl)-benzyl)-1,6-dihydropyrimidine-4-carboxylate (**11**).* Off-white solid (45%): R_f = 0.53 (EtOAc/hexane = 1/1); ^{1}H NMR (300 MHz, $CDCl_3$) δ 8.20 (d, J = 8.4 Hz, 2H), 7.74 (d, J = 7.8 Hz, 1H), 7.65 (t, J = 7.9 Hz, 1H), 7.51 (t, J = 7.2 Hz, 2H), 7.42 (t, J = 7.3 Hz, 1H), 7.13 (d, J = 7.5 Hz, 1H), 4.44 (s, 2H), 3.89 (q, J = 7.2 Hz, 2H), 3.84 (s, 3H), 1.23 (t, J = 7.2 Hz, 3H); ^{13}C NMR (75 MHz, $CDCl_3$) δ 163.8, 163.3, 158.3, 156.2, 140.7, 138.1, 134.2, 133.2, 132.7, 130.7, 129.3, 128.8, 128.4, 128.0, 127.9, 126.7 (q), 126.2, 122.6, 53.3, 41.2, 38.3, 13.2; LRMS (ESI) m/z 461 [M + H$^+$].

*Methyl 5-(Benzoyloxy)-2-benzyl-1-methyl-6-oxo-1,6-dihydropyrimidine-4-carboxylate (**12**).* Off-white solid (61%): R_f = 0.35 (EtOAc/hexane = 1/1); ^{1}H NMR (300 MHz, $CDCl_3$) δ 8.18 (d, J = 7.8 Hz, 2H), 7.63 (t, J = 7.8 Hz, 1H), 7.49 (t, J = 7.8 Hz, 2H), 7.36−7.21 (m, 5H), 4.25 (s, 2H), 3.85 (s, 3H), 3.44 (s, 3H); ^{13}C NMR (75 MHz, $CDCl_3$) δ 163.7, 163.3, 158.7, 157.7, 140.7, 137.5, 134.1, 133.7, 130.6, 129.3, 128.7, 128.4, 127.7, 53.2, 42.5, 32.0; LRMS (ESI) m/z 379 [M + H$^+$].

*Methyl 5-(Benzoyloxy)-2-ethyl-1-methyl-6-oxo-1,6-dihydropyrimidine-4-carboxylate (**13**).* Off-white solid (97%): R_f = 0.25

DOI: 10.1021/acs.jmedchem.8b00883
J. Med. Chem. 2018, 61, 9952−9965

(EtOAc/hexane = 3/2); ^{1}H NMR (300 MHz, $CDCl_3$) δ 8.16 (J = 7.8 Hz, 2H), 7.61 (t, J = 7.5 Hz, 1H), 7.47 (t, J = 7.5 Hz, 2H), 3.80 (s, 3H), 3.57 (s, 3H), 2.82 (q, J = 7.3 Hz, 2H), 1.35 (t, J = 7.3 Hz, 3H); ^{13}C NMR (75 MHz, $CDCl_3$) δ 163.76, 163.5, 160.3, 158.6, 140.9, 136.7, 134.0, 130.6, 128.6, 128.4, 53.1, 31.4, 28.9, 10.8; LRMS (ESI) m/z 317 [M + H$^+$].

*Synthesis of Methyl 5-(Benzoyloxy)-1-methyl-6-oxo-2-(1-(2-(trifluoromethyl)phenyl)ethyl)-1,6-dihydropyrimidine-4-carboxylate (**14**).* To a solution of **7** (1.0 equiv) in anhydrous THF (0.2 M) were added Cs_2CO_3 (3.0 equiv) and MeI (5.0 equiv). The reaction mixture was stirred overnight at 40 °C. The reaction mixture was diluted with EtOAc and washed with 1 N HCl and brine. The organic layer was dried over Na_2SO_4 and evaporated in vacuo. The crude mixture was purified by flash column chromatography (EtOAc/hexane = 2/3) to obtain the desired product as an off-white solid (58%): R_f = 0.65 (EtOAc/hexane = 1/1); ^{1}H NMR (300 MHz, $CDCl_3$) δ 8.19 (d, J = 7.8 Hz, 2H), 7.74 (d, J = 7.8 Hz, 1H), 7.64 (t, J = 7.2 Hz, 1H), 7.50 (t, J = 7.5 Hz, 2H), 7.40 (t, J = 7.5 Hz, 1H), 7.27 (d, J = 7.2 Hz, 1H), 4.60 (q, J = 6.6 Hz, 1H), 3.86 (s, 3H), 3.35 (s, 3H), 1.72 (d, J = 6.6 Hz, 3H); LRMS (ESI) m/z 461 [M + H$^+$].

*Synthesis of Methyl 5-(Benzoyloxy)-6-methoxy-2-(2-(trifluoromethyl)benzyl)pyrimidine-4-carboxylate (**15**).* To a solution of **7** (1.0 equiv) in anhydrous DMF (0.2 M) was added K_2CO_3 (2.0 equiv) and MeI (3.0 equiv). The reaction mixture was stirred at rt for 4 h. The reaction mixture was diluted with EtOAc, and washed with 1 N HCl and brine. The organic layer was dried over Na_2SO_4 and evaporated in vacuo. The crude mixture was purified by flash column chromatography (EtOAc/hexane = 1/9 → 1/4 → 2/3) to obtain two different isomers, the desired product (**15**, *O*-Me, 11%) and **10** (*N*-Me, 83%): R_f = 0.31 (EtOAc/hexane = 1/4); ^{1}H NMR (300 MHz, $CDCl_3$) δ 8.18 (d, J = 7.8 Hz, 2H), 7.66 (t, J = 7.4 Hz, 1H), 7.55−7.46 (m, 3H), 7.40−7.33 (m, 2H), 4.50 (s, 2H), 3.87 (s, 3H), 3.84 (s, 3H); ^{13}C NMR (75 MHz, $CDCl_3$) δ 165.5, 163.9, 163.8, 163.3, 146.9, 136.2, 134.2, 132.3, 132.1, 131.8, 130.6, 128.9, 128.4, 126.9, 126.5, 126.1 (q), 122.8, 55.0, 53.3, 41.6; LRMS (ESI) m/z 447 [M + H$^+$].

*Synthesis of Methyl 5-Hydroxy-1-methyl-6-oxo-2-(2-(trifluoromethyl)benzyl)-1,6-dihydropyrimidine-4-carboxylate (**16**).* To a solution of **10** (1.0 equiv) in anhydrous MeOH (0.2 M) was added *N*-benzylmethylamine (2.0 equiv). The reaction mixture was refluxed for 2 h. The reaction mixture was diluted with EtOAc and washed with 1 N HCl and brine. The organic layer was dried over $MgSO_4$ and evaporated in vacuo. The crude mixture was suspended in EtOH and stirred for about 2 h. The solid was filtered and washed with EtOH and Et_2O to obtain the desired product as an off-white solid (84%): R_f = 0.28 (MeOH/CH_2Cl_2 = 5/95); ^{1}H NMR (300 MHz, $CDCl_3$) δ 10.58 (bs, 1H), 7.71 (d, J = 7.2 Hz, 1H), 7.45 (t, J = 7.5 Hz, 1H), 7.38 (t, J = 7.5 Hz, 1H), 6.95 (d, J = 7.8 Hz, 1H), 4.36 (s, 2H), 4.01 (s, 3H), 3.33 (s, 3H); ^{13}C NMR (75 MHz, $CDCl_3$) δ 169.7, 158.7, 149.1, 148.9, 133.5, 132.7, 128.5, 128.1, 127.7, 126.8 (q), 126.2, 124.4, 122.5, 53.6, 38.7, 31.9; LRMS (ESI) m/z 343 [M + H$^+$].

*Synthesis of Methyl 5-Methoxy-1-methyl-6-oxo-2-(2-(trifluoromethyl)benzyl)-1,6-dihydropyrimidine-4-carboxylate (**17**).* To a solution of **16** (1.0 equiv) in anhydrous $CHCl_3$/MeOH (2/1, 0.2 M) was added trimethylsilyldiazomethane (5.5 equiv, 1.1 equiv, 5 times) portionwise for about 1 h. The reaction mixture was stirred overnight at rt. The reaction mixture was evaporated in vacuo and suspended in EtOH. After being stirred for 2 h, the solid was filtered and washed with EtOH and Et_2O to obtain the desired product as an off-white solid (80%): R_f = 0.24 (EtOAc/hexane = 2/3); ^{1}H NMR (300 MHz, $CDCl_3$) δ 7.70 (d, J = 7.8 Hz, 1H), 7.46 (t, J = 7.2 Hz, 1H), 7.38 (t, J = 7.5 Hz, 1H), 7.00 (d, J = 7.5 Hz, 1H), 4.35 (s, 2H), 4.01 (s, 3H), 3.92 (s, 3H), 3.32 (s, 3H); ^{13}C NMR (75 MHz, $CDCl_3$) δ 164.6, 160.1, 153.7, 144.1, 139.9, 133.1, 132.7, 128.8, 128.5, 128.1, 127.7, 126.7 (q), 126.1, 122.5, 60.7, 53.0, 38.8, 31.5; LRMS (ESI) m/z 357 [M + H$^+$].

*General Procedure of Thermal Addition and Elimination Reactions (**P01**−**P17**).* To a solution of starting material (1.0 equiv) in anhydrous MeOH (0.2 M) was added each amine (3.0 equiv or 2.2 equiv in the case of **P16**). The reaction mixture was refluxed until completion of reaction (TLC or LC-MS). In most cases, overnight reflux was enough to complete the reaction, except with **P05** (3 days), **P12** (5 days), and **P16** (30 min). The reaction mixture was diluted with EtOAc and washed with 1 N HCl and brine. The organic layer was dried over $MgSO_4$ and evaporated in vacuo. The crude mixture was suspended in EtOH or Et_2O for crystallization of each desired product.

*N-Benzyl-5-hydroxy-1-methyl-6-oxo-2-(2-(trifluoromethyl)-benzyl)-1,6-dihydropyrimidine-4-carboxamide (**P01**).* Off-white solid (83%): mp = 131.7 °C; R_f = 0.54 (MeOH/$CHCl_3$ = 1/9); ^{1}H NMR (300 MHz, $CDCl_3$) δ 12.00 (s, 1H), 7.67 (d, J = 7.2 Hz, 2H), 7.41 (t, J = 7.3 Hz, 1H), 7.35−7.29 (m, 4H), 7.23−7.21 (m, 2H), 7.03 (d, J = 7.5 Hz, 1H), 4.49 (d, J = 6.0 Hz, 2H), 4.21 (s, 2H), 3.41 (s, 3H); ^{13}C NMR ($CDCl_3$, 75 MHz) δ 167.9, 158.8, 148.4, 146.9, 136.9, 133.3, 132.3, 130.1, 128.8, 128.7, 128.3, 127.83, 127.78, 127.6, 126.5 (q), 126.1, 125.1, 122.5, 43.1, 38.1, 31.3; HRMS (ESI) m/z calcd for $C_{21}H_{19}F_3N_3O_3$ [M + H]$^+$ 418.1379, found 418.1382.

*N,2-Dibenzyl-5-hydroxy-1-methyl-6-oxo-1,6-dihydropyrimidine-4-carboxamide (**P02**).* Off-white solid (87%): R_f = 0.32 (MeOH/$CHCl_3$ = 1/9); ^{1}H NMR (300 MHz, $CDCl_3$) δ 12.01 (s, 1H), 7.89 (bs, 1H), 7.36−7.24 (m, 8H), 7.10 (d, J = 6.9 Hz, 2H), 4.58 (d, J = 6.0 Hz, 2H), 4.04 (s, 2H), 3.42 (s, 3H); ^{13}C NMR (75 MHz, $CDCl_3$) δ 168.3, 159.0, 149.4, 147.1, 137.2, 134.6, 129.1, 129.0, 128.3, 127.9, 127.6, 125.3, 43.2, 41.8, 31.7; LRMS (ESI) m/z 350 [M + H]$^+$.

*N-Benzyl-2-ethyl-5-hydroxy-1-methyl-6-oxo-1,6-dihydropyrimidine-4-carboxamide (**P03**).* Off-white solid (80%): R_f = 0.44 (MeOH/$CHCl_3$ = 1/9); ^{1}H NMR (300 MHz, $CDCl_3$) δ 11.93 (s, 1H), 7.98 (bs, 1H), 7.40−7.31 (m, 5H), 4.62 (d, J = 6.3 Hz, 2H), 3.54 (s, 3H), 2.68 (q, J = 7.2 Hz, 2H), 1.27 (t, J = 7.2 Hz, 3H); ^{13}C NMR (75 MHz, $CDCl_3$) δ 168.5, 158.9, 151.8, 146.7, 137.5, 129.0, 127.9, 127.7, 125.2, 43.1, 31.0, 27.8, 10.7; LRMS (ESI) m/z 288 [M + H]$^+$.

*N-Benzyl-1-ethyl-5-hydroxy-6-oxo-2-(2-(trifluoromethyl)benzyl)-1,6-dihydropyrimidine-4-carboxamide (**P04**).* Off-white solid (73%); R_f = 0.57 (MeOH/$CHCl_3$ = 1/9); ^{1}H NMR (300 MHz, $CDCl_3$) δ 11.93 (s, 1H), 7.65 (d, J = 8.1 Hz, 1H), 7.52 (bs, 1H), 7.44−7.30 (m, 5H), 7.24−7.21 (m, 2H), 7.06 (d, J = 7.8 Hz, 1H), 4.50 (d, J = 6.0 Hz, 2H), 4.23 (s, 2H), 3.97 (q, J = 7.5 Hz, 2H), 1.28 (t, J = 7.5 Hz, 3H); ^{13}C NMR (75 MHz, $CDCl_3$) δ 168.1, 158.6, 148.1, 147.4, 137.1, 133.9, 132.3, 130.7, 129.1, 128.8, 128.5, 128.1, 128.0, 127.8, 126.7 (q), 126.3, 152.2, 122.7, 43.3, 40.4, 37.7, 13.5; HRMS (ESI) m/z calcd for $C_{22}H_{21}N_3O_3F_3$ [M + H]$^+$ 432.1535, found 432.1540.

*5-Hydroxy-1-methyl-6-oxo-N-phenyl-2-(2-(trifluoromethyl)-benzyl)-1,6-dihydropyrimidine-4-carboxamide (**P05**).* Off-white solid (59%): R_f = 0.45 (MeOH/$CHCl_3$ = 1/9); ^{1}H NMR (300 MHz, $CDCl_3$) δ 11.78 (s, 1H), 9.04 (s, 1H), 7.79 (d, J = 7.5 Hz, 1H), 7.61−7.45 (m, 4H), 7.35 (t, J = 7.9 Hz, 2H), 7.21−7.13 (m, 2H), 4.30 (s, 2H), 3.53 (s, 3H); ^{13}C NMR (75 MHz, $CDCl_3$) δ 166.1, 158.7, 148.7, 147.4, 136.4, 133.5, 132.4, 131.0, 129.3, 127.9, 126.8 (q), 126.2, 125.3, 125.2, 122.6, 119.8, 38.2, 31.5; LRMS (ESI) m/z 404 [M + H]$^+$.

*N-(Cyclohexylmethyl)-5-hydroxy-1-methyl-6-oxo-2-(2-(trifluoromethyl)benzyl)-1,6-dihydropyrimidine-4-carboxamide (**P06**).* Off-white solid (89%): R_f = 0.57 (MeOH/$CHCl_3$ = 1/9); ^{1}H NMR (300 MHz, $CDCl_3$) δ 12.11 (s, 1H), 7.73 (d, J = 7.5 Hz, 1H), 7.53 (t, J = 7.5 Hz, 1H), 7.44 (t, J = 7.5 Hz, 1H), 7.30 (bs, 1H), 7.12 (d, J = 7.5 Hz, 1H), 4.25 (s, 2H), 3.49 (s, 3H), 3.15 (t, J = 6.5 Hz, 2H), 1.73−1.58 (m, 5H), 1.50−1.35 (m, 1H), 1.29−1.10 (m, 3H), 0.92−0.81 (m, 2H); ^{13}C NMR (75 MHz, $CDCl_3$) δ 168.1, 159.0, 148.3, 146.9, 133.6, 132.3, 130.8, 129.1, 128.7, 127.7, 126.6 (q), 126.2, 125.3, 122.6, 45.2, 38.3, 37.8, 31.4, 30.8, 26.4, 25.9; LRMS (ESI) m/z 424 [M + H]$^+$.

*5-Hydroxy-1-methyl-6-oxo-N-(pyridin-2-ylmethyl)-2-(2-(trifluoromethyl)benzyl)-1,6-dihydropyrimidine-4-carboxamide (**P07**).* Off-white solid (82%): R_f = 0.26 (MeOH/$CHCl_3$ = 1/9); ^{1}H NMR (300 MHz, $CDCl_3$) δ 12.09 (bs, 1H), 8.54 (d, J = 4.2 Hz, 1H), 8.44 (bs, 1H), 7.73−7.66 (m, 2H), 7.49 (t, J = 7.5 Hz, 1H), 7.41 (t, J = 7.5 Hz, 1H), 7.28−7.22 (m, 2H), 7.09 (d, J = 7.5 Hz, 1H), 4.66 (d, J = 5.7 Hz, 2H), 4.27 (s, 2H), 3.43 (s, 3H); ^{13}C NMR (75 MHz,

DOI: 10.1021/acs.jmedchem.8b00883
J. Med. Chem. 2018, 61, 9952−9965

$CDCl_3$) δ 168.4, 159.0, 155.5, 149.2, 148.4, 147.2, 137.2, 133.5, 132.5, 130.1, 128.8, 128.4, 127.7, 126.6 (q), 126.2, 125.4, 122.8, 122.6, 122.3, 44.1, 38.3, 31.5; HRMS (ESI) m/z calcd for $C_{20}H_{18}N_4O_3F_3$ $[M + H]^+$ 419.1331, found 419.1324.

5-Hydroxy-1-methyl-6-oxo-N-(pyridin-3-ylmethyl)-2-(2-(trifluoromethyl)benzyl)-1,6-dihydropyrimidine-4-carboxamide (**P08**). Off-white solid (79%): R_f = 0.22 (MeOH/$CHCl_3$ = 1/9); ^{1}H NMR (300 MHz, $CDCl_3$) δ 11.82 (bs, 1H), 8.56–8.51 (m, 2H), 7.66 (d, J = 7.5 Hz, 2H), 7.60 (d, J = 7.8 Hz, 1H), 7.43 (t, J = 7.2 Hz, 1H), 7.35 (t, J = 7.2 Hz, 1H), 7.30–7.26 (m, 1H), 7.01 (d, J = 7.8 Hz, 1H), 4.52 (d, J = 6.0 Hz, 2H), 4.22 (s, 2H), 3.42 (s, 3H); ^{13}C NMR (75 MHz, $CDCl_3$) δ 168.2, 158.8, 149.4, 149.3, 148.6, 147.1, 135.7, 133.4, 132.8, 132.4, 130.0, 128.8, 128.4, 127.8, 126.6 (q), 126.1, 125.0, 123.8, 122.5, 40.7, 38.2, 31.5; LRMS (ESI) m/z 419 $[M + H]^+$.

N-(2-Fluorobenzyl)-5-hydroxy-1-methyl-6-oxo-2-(2-(trifluoromethyl)benzyl)-1,6-dihydropyrimidine-4-carboxamide (**P09**). Off-white solid (86%): R_f = 0.40 (MeOH/$CHCl_3$ = 1/9); ^{1}H NMR (300 MHz, $CDCl_3$) δ 11.91 (s, 1H), 7.68 (d, J = 7.5 Hz, 1H), 7.63 (bs, 1H), 7.46 (t, J = 7.2 Hz, 1H), 7.38 (t, J = 7.2 Hz, 1H), 7.33–7.28 (m, 2H), 7.14–7.04 (m, 3H), 4.55 (d, J = 6.3 Hz, 2H), 4.23 (s, 2H), 3.44 (s, 3H); ^{13}C NMR (75 MHz, $CDCl_3$) δ 168.1, 162.8, 159.5, 158.9, 148.5, 147.0, 133.4, 132.3, 130.4, 130.3, 129.9, 129.8, 128.8, 128.4, 127.7, 126.6 (q), 126.2, 125.1, 124.5 (d), 124.2, 124.1, 122.6, 115.8, 115.5, 38.2, 37.3, 31.5; HRMS (ESI) m/z calcd for $C_{21}H_{18}N_3O_3F_4$ $[M + H]^+$ 436.1284, found 436.1282.

N-(4-Fluorobenzyl)-5-hydroxy-1-methyl-6-oxo-2-(2-(trifluoromethyl)benzyl)-1,6-dihydropyrimidine-4-carboxamide (**P10**). Off-white solid (79%): R_f = 0.46 (MeOH/$CHCl_3$ = 1/9); ^{1}H NMR (300 MHz, $CDCl_3$) δ 11.93 (s, 1H), 7.67 (d, J = 7.5 Hz, 1H), 7.59 (bs, 1H), 7.43 (t, J = 7.2 Hz, 1H), 7.35 (t, J = 7.2 Hz, 1H), 7.24–7.19 (m, 2H), 7.05–7.00 (m, 3H), 4.47 (d, J = 6.3 Hz, 2H), 4.23 (s, 2H), 3.43 (s, 3H); ^{13}C NMR (75 MHz, $CDCl_3$) δ 168.1, 164.2, 160.9, 158.9, 148.6, 147.2, 133.6, 133.0 (d), 132.4, 130.2, 129.8, 129.7, 128.9, 128.5, 127.8, 126.7 (q), 126.3, 125.2, 122.6, 116.1, 115.8, 42.6, 38.4, 31.6; LRMS (ESI) m/z 436 $[M + H]^+$.

N-(Benzo[d][1,3]dioxol-5-ylmethyl)-5-hydroxy-1-methyl-6-oxo-2-(2-(trifluoromethyl)benzyl)-1,6-dihydropyrimidine-4-carboxamide (**P11**). Pale-yellow solid (61%): R_f = 0.36 (MeOH/$CHCl_3$ = 1/9); ^{1}H NMR (300 MHz, $CDCl_3$) δ 7.68 (d, J = 7.5 Hz, 1H), 7.54 (bs, 1H), 7.44 (t, J = 7.5 Hz, 1H), 7.37 (t, J = 7.2 Hz, 1H), 7.02 (d, J = 7.2 Hz, 1H), 6.78–6.69 (m, 3H), 5.96 (s, 2H), 4.40 (d, J = 6.0 Hz, 2H), 4.22 (s, 2H), 3.43 (s, 3H); ^{13}C NMR (75 MHz, $CDCl_3$) δ 167.9, 158.9, 148.4, 148.1, 147.4, 147.1, 133.5, 132.4, 130.8, 130.1, 128.8, 128.4, 127.7, 126.6 (q), 126.2, 125.1, 122.5, 121.3, 108.5, 108.4, 101.3 (t), 43.1, 38.2, 31.5; LRMS (ESI) m/z 462 $[M + H]^+$.

N-Benzyl-5-hydroxy-N,1-dimethyl-6-oxo-2-(2-(trifluoromethyl)benzyl)-1,6-dihydropyrimidine-4-carboxamide (Rotameric Mixture, **P12**). Pale-yellow solid (43%): R_f = 0.54 (MeOH/$CHCl_3$ = 1/9); ^{1}H NMR (300 MHz, $(CD_3)_2CO$) δ 11.48 (s, 0.5H) c, 10.84 (s, 0.5H), 7.78 (d, J = 7.8 Hz, 1H), 7.64–7.56 (m, 1H), 7.49–7.26 (m, 6H), 7.10–7.09 (m, 1H), 4.76 (s, 1H), 4.64 (s, 1H), 4.39 (s, 1H), 4.32 (s, 1H), 3.61 (s, 1.5H), 3.58 (s, 1.5H), 2.79 (s, 3H); ^{13}C NMR (75 MHz, $(CD_3)_2CO$) δ 168.4, 159.6, 149.6, 149.5, 146.1, 145.2, 138.2, 137.9, 135.5, 135.0, 133.3, 133.2, 132.8, 130.9, 129.4, 129.2, 128.5, 128.4, 128.3, 128.2, 128.1, 126.8, 122.5, 54.4, 51.8, 38.6, 38.4, 36.6, 34.1, 31.2; LRMS (ESI) m/z 432 $[M + H]^+$.

5-Hydroxy-1-methyl-6-oxo-N-(1-phenylethyl)-2-(2-(trifluoromethyl)benzyl)-1,6-dihydropyrimidine-4-carboxamide (**P13**). Pale-yellow solid (67%): R_f = 0.49 (MeOH/$CHCl_3$ = 1/9); ^{1}H NMR (300 MHz, $CDCl_3$) δ 7.71 (d, J = 7.5 Hz, 1H), 7.49 (t, J = 7.8 Hz, 2H), 7.43–7.26 (m, 4H), 7.22–7.19 (m, 2H), 7.10 (d, J = 7.2 Hz, 1H), 5.10 (quint, J = 6.9 Hz, 1H), 4.24 (s, 2H), 3.47 (s, 3H), 1.47 (d, J = 6.9 Hz, 3H); ^{13}C NMR (75 MHz, $CDCl_3$) δ 167.2, 158.9, 148.4, 146.9, 142.3, 133.6, 132.2, 130.7, 129.0, 128.9, 128.6, 127.8, 127.7, 126.6 (q), 126.2, 126.0, 125.2, 122.6, 48.9, 38.2, 31.4, 22.1; LRMS (ESI) m/z 432 $[M + H]^+$.

N-Benzyl-5-hydroxy-6-oxo-2-(2-(trifluoromethyl)benzyl)-1,6-dihydropyrimidine-4-carboxamide (**P14**). Off-white solid (78%): R_f = 0.23 (MeOH/$CHCl_3$ = 1/9); ^{1}H NMR (300 MHz, $(CD_3)_2SO$) δ 12.35 (bs, 1H), 8.87 (t, J = 5.8 Hz, 1H), 7.73 (d, J = 7.7 Hz, 1H), 7.59 (t, J = 7.5 Hz, 1H), 7.47 (t, J = 7.7 Hz, 1H), 7.35–7.24 (m, 6H), 4.43 (d, J = 6.3 Hz, 1H), 4.10 (s, 2H); ^{13}C NMR (75 MHz, $(CD_3)_2SO$) δ 168.3, 158.1, 148.0, 147.7, 138.3, 134.7, 132.7, 130.9, 128.4, 127.4, 127.3, 127.2, 127.1, 126.8, 126.2, 125.9 (q), 122.6, 42.2, 36.4; LRMS (ESI) m/z 404 $[M + H]^+$.

N-Benzyl-5-hydroxy-1-methyl-6-oxo-2-(1-(2-(trifluoromethyl)-phenyl)ethyl)-1,6-dihydropyrimidine-4-carboxamide (**P15**). Off-white solid (80%): R_f = 0.63 (MeOH/= 1/9); ^{1}H NMR (300 MHz, $CDCl_3$) δ 12.05 (s, 1H), 7.90 (bs, 1H), 7.72 (d, J = 7.2 Hz, 1H), 7.44–7.33 (m, 7H), 7.06 (d, J = 7.5 Hz, 1H), 4.65 (q, J = 3.1 Hz, 2H), 4.53 (q, J = 6.6 Hz, 1H), 3.31 (s, 3H), 1.61 (d, J = 6.6 Hz, 3H); ^{13}C NMR (75 MHz, $CDCl_3$) δ 168.5, 159.0, 151.7, 147.3, 140.2, 137.3, 132.9, 129.1, 128.0, 127.9, 127.8, 127.5, 127.0 (q), 126.4, 124.7, 122.7, 43.3, 40.2, 30.8, 21.8; LRMS (ESI) m/z 432 $[M + H]^+$.

N-Benzyl-5-hydroxy-6-methoxy-2-(2-(trifluoromethyl)benzyl)-pyrimidine-4-carboxamide (**P16**). Pale-yellow solid (60%): R_f = 0.64 (only CH_2Cl_2); ^{1}H NMR (300 MHz, $CDCl_3$) δ 11.77 (s, 1H), 8.17 (bs, 1H), 7.64 (d, J = 7.8 Hz, 1H), 7.46–7.26 (m, 8H), 4.58 (d, J = 6.0 Hz, 2H), 4.29 (s, 2H), 3.98 (s, 3H); ^{13}C NMR (75 MHz, $CDCl_3$) δ 168.0, 160.9, 156.4, 142.2, 137.1, 136.8, 133.2, 132.1, 131.6, 129.0, 127.9, 127.7, 126.7, 126.4, 126.0 (q), 122.8, 54.7, 43.1, 41.0; LRMS (ESI) m/z 418 $[M + H]^+$.

N-Benzyl-5-methoxy-1-methyl-6-oxo-2-(2-(trifluoromethyl)-benzyl)-1,6-dihydropyrimidine-4-carboxamide (**P17**). Pale-yellow solid (91%): R_f = 0.69 (MeOH/$CHCl_3$ = 1/9); ^{1}H NMR (300 MHz, $CDCl_3$) δ 7.61 (d, J = 7.5 Hz, 1H), 7.51 (bs, 1H), 7.39–7.26 (m, 5H), 7.18 (d, J = 7.5 Hz, 2H), 7.05 (d, J = 7.8 Hz, 1H), 4.45 (d, J = 5.7 Hz, 2H), 4.24 (s, 2H), 4.01 (s, 3H), 3.42 (s, 3H); ^{13}C NMR (75 MHz, $CDCl_3$) δ 162.3, 160.7, 152.6, 144.6, 138.7, 137.9, 133.0, 132.2, 130.5, 128.7, 128.4, 127.9, 127.7, 127.6, 126.5 (q), 126.1, 122.5, 61.0, 43.5, 38.4, 31.3; LRMS (ESI) m/z 432 $[M + H]^+$.

Synthesis of P18. *Synthesis of 5-(Benzyloxy)-1-methyl-6-oxo-2-(2-(trifluoromethyl)benzyl)-1,6-dihydropyrimidine-4-carboxylic Acid* (**18**). To a solution of **9** (1.0 equiv) in anhydrous DMF (0.2 M) were added K_2CO_3 (3.0 equiv), KI (0.3 equiv), and benzyl bromide (3.0 equiv). The reaction mixture was heated overnight at 80 °C. The reaction mixture was diluted in EtOAc and washed with 1 N HCl and brine. The organic layer was dried over $MgSO_4$ and evaporated in vacuo. The crude mixture was dissolved in MeOH (0.1 M). A 5 M NaOH solution (20% MeOH) was added to the reaction mixture, and then it was stirred at rt for 5 h. The reaction mixture was evaporated in vacuo, then diluted in EtOAc, and washed with 1 N HCl and brine. The separated organic layer was dried under $MgSO_4$ and evaporated in vacuo. The crude mixture was suspended in EtOH. After being stirred for 2 h, the solid was filtered and washed with EtOH and Et_2O to obtain the desired product as an off-white solid (55%): R_f = 0.06 (only EtOAc); ^{1}H NMR (300 MHz, $CDCl_3$) δ 7.73 (d, J = 7.8 Hz, 1H), 7.54–7.42 (m, 4H), 7.38–7.31 (m, 3H), 7.05 (d, J = 7.5 Hz, 1H), 5.47 (s, 2H), 4.29 (s, 2H), 3.45 (s, 3H); ^{13}C NMR (75 MHz, $CDCl_3$) δ 161.6, 160.1, 153.4, 144.8, 135.9, 135.0, 132.6, 132.4, 130.3, 129.0, 128.9, 128.8, 128.6, 128.5, 128.2, 126.9 (q), 126.1, 122.5, 75.1, 38.3, 31.6; LRMS (ESI) m/z 419 $[M + H]^+$.

Synthesis of 5-(Benzyloxy)-N-methoxy-N,1-dimethyl-6-oxo-2-(2-(trifluoromethyl)benzyl)-1,6-dihydropyrimidine-4-carboxamide (**19**). To a solution of **18** (1.0 equiv) in anhydrous DMF (0.2 M) was added dropwise a CDI (1.1 equiv) solution in anhydrous CH_2Cl_2 (0.5 M) at 0–5 °C. After being stirred for 1 h at 0–5 °C, *N,O*-dimethylhydroxylamine hydrochloride (1.1 equiv) and TEA (1.2 equiv) were added to the reaction mixture sequentially at the same temperature. After being stirred overnight at rt, the reaction mixture was diluted in EtOAc and washed with 1 N HCl and brine. The organic layer was dried over Na_2SO_4 and evaporated in vacuo. The crude mixture was purified by flash column chromatography (EtOAc/hexane = 4/1) to obtain the desired product as an off-white solid (61%): R_f = 0.26 (EtOAc/hexane = 1/1); ^{1}H NMR (300 MHz, $CDCl_3$) δ 7.70 (d, J = 7.5 Hz, 1H), 7.51–7.29 (m, 7H), 7.08 (d, J = 7.5 Hz, 1H), 5.24 (s, 2H), 4.32 (s, 2H), 3.51 (s, 3H), 3.42 (s, 3H), 3.27 (s, 3H); ^{13}C NMR (75 MHz, $CDCl_3$) δ 165.7, 159.8, 154.3, 145.6, 139.7, 137.0, 133.2, 132.5, 129.8, 128.9, 128.5, 128.4, 128.2, 127.7, 126.5 (q), 126.2, 122.5, 74.3, 61.8, 38.6, 31.8, 31.2; LRMS (ESI) m/z 462 $[M + H]^+$.

DOI: 10.1021/acs.jmedchem.8b00883
J. Med. Chem. 2018, 61, 9952–9965

*Synthesis of 5-(Benzyloxy)-3-methyl-6-(3-phenylpropanoyl)-2-(2-(trifluoromethyl)benzyl)pyrimidin-4(3H)-one (**20**).* Mg turnings (2.5 equiv) was suspended into anhydrous THF (1 M) and then heated to 40 °C. A few drops of 1,2-dibromoethane was added to activate the Mg. To a solution of (5-chloro-1-pentynyl)trimethylsilane (2.0 equiv) in anhydrous THF (1 M) was added 1,2-dibromoethane (total of 0.2 equiv). This solution was added slowly to the Mg solution, and then the reaction mixture was stirred overnight at 40 °C (Grignard reagent). To a solution of **19** (1.0 equiv) in anhydrous THF (0.5 M) was added dropwise Grignard reagent at 0−5 °C. After being stirred at rt for 2 h, the reaction mixture was quenched with aqueous NH_4Cl and then extracted with EtOAc. The organic layer was washed with brine, dried over Na_2SO_4, and evaporated in vacuo. The crude mixture was purified by flash column chromatography (EtOAc/hexane = 1/4 → 1/3) to obtain the desired product as an off-white solid (75%): R_f = 0.63 (EtOAc/hexane = 1/1); ^{1}H NMR (300 MHz, $CDCl_3$) δ 7.70 (d, J = 7.5 Hz, 1H), 7.47−7.18 (m, 10H), 7.10 (d, J = 6.9 Hz, 2H), 7.06 (d, J = 7.5 Hz, 1H), 5.30 (s, 2H), 4.27 (s, 2H), 3.43 (s, 3H), 2.97 (t, J = 6.9 Hz, 2H), 2.86 (t, J = 6.9 Hz, 2H); ^{13}C NMR (75 MHz, $CDCl_3$) δ 199.8, 160.6, 153.3, 144.7, 140.9, 136.4, 133.2, 132.3, 130.2, 129.0, 128.9, 128.6, 128.5, 128.4, 128.3, 127.6, 126.5 (q), 126.1, 126.0, 122.5, 74.4, 42.2, 38.4, 31.2, 29.4; LRMS (ESI) m/z 507 $[M + H]^+$.

*Synthesis of 5-Hydroxy-3-methyl-6-(3-phenylpropanoyl)-2-(2-(trifluoromethyl)benzyl)pyrimidin-4(3H)-one (**P18**).* To a solution of **20** in MeOH/THF (3/1, 0.2 M) was added 10% Pd/C. After being stirred at rt for 1 h under H_2 atmosphere, the reaction mixture was filtered through a Celite pad and evaporated in vacuo. The crude mixture was purified by flash column chromatography (MeOH/CH_2Cl_2 = 2/98 → 5/95) to obtain the desired product as a pale-yellow solid (71%): R_f = 0.54 (MeOH/$CHCl_3$ = 1/9); ^{1}H NMR ($CDCl_3$, 300 MHz) δ 7.71 (d, J = 7.2 Hz, 1H), 7.46 (t, J = 7.2 Hz, 1H), 7.38 (t, J = 7.2 Hz, 1H), 7.29−7.16 (m, 3H), 7.11−7.07 (m, 3H), 4.26 (s, 2H), 3.45 (s, 3H), 3.18 (t, J = 7.5 Hz, 2H), 2.89 (t, J = 7.5 Hz, 2H); ^{13}C NMR ($CDCl_3$, 75 MHz) δ 208.1, 159.6, 148.3, 140.7, 133.7, 132.3, 130.4, 129.3, 128.7, 128.5, 128.4, 127.6, 126.6 (q), 126.3, 122.6, 39.6, 38.3, 31.5, 29.8; LRMS (ESI) m/z 417 $[M + H]^+$.

Biology. *Strains and Media.* *Mtb* H37Rv or mutants thereof were used for all experiments. Liquid media were either Middlebrook 7H9 based or GAST, whereas solid agar medium consisted of Middlebrook 7H11 supplemented with bovine serum albumin fraction V (5 g/L)/dextrose (2 g/L)/NaCl (0.81 g/L)/0.5% glycerol/0.06% oleic acid. Middlebrook 7H9/ADC consisted of Middlebrook 7H9 broth (Becton Dickinson) supplemented with bovine serum albumin fraction V (5 g/L)/dextrose (2 g/L)/NaCl (0.81 g/L)/0.2% glycerol/0.05% Tween 80. Glycerol/alanine/salts with Tween 80 (GAST) was used as the defined liquid medium.[44] Glucose medium (GBSA) contained bovine serum albumin fraction V (5 g/L)/dextrose (4 g/L)/NaCl (0.81 g/L)/0.05% Tyloxapol. Dipalmitoylphosphatidyl choline (DPPC) medium (DBSA) contained bovine serum albumin fraction V (5 g/L)/DPPC (5 mg/L)/cholesterol (24 mg/L)/NaCl (0.81 g/L)/0.05% Tyloxapol. Cholesterol medium (Chol) contained bovine serum albumin fraction V (5 g/L)/cholesterol (97 mg/L)/NaCl (0.81 g/L)/0.05% Tyloxapol. The low-pH, nitrosative-stress medium contained bovine serum albumin fraction V (5 g/L)/butyric acid (2.5 mM)/$NaNO_2$ (6.9 mg/mL)/NaCl (0.81 g/L)/0.05% Tyloxapol and was pH adjusted to 6.0. MIC determination was performed as previously described.[45]

Screening of St. Jude's Pyrimidinedione Library. The 6207-compound pyrimidinedione library was kindly provided St. Jude Children's Research Hospital, Inc., and it was screened in a single-point assay at 10 μM final concentration Middlebrook 7H9/ADC in 384-well plates (Greiner plates, catalogue no. 781091) containing 25 μL of *Mtb* expressing GFP from pMSP12 (Addgene plasmid #30167). Rifampicin and isoniazid were used as positive controls. Growth was measured by fluorescence after 3 days of incubation. Thirty-eight hits were selected for follow-up on the basis of >50% inhibition of *Mtb* growth and z-scores of <−3. The selected hits were followed up in duplicate 12-point MIC determinations in GAST with Mg^{2+} concentrations adjusted to 0.06, 6, and 60 mM. Growth was measured using an inverted enlarging mirror at 1, 2, and 3 weeks with the MIC taken as the concentration that completely inhibited all visible growth.

Efficacy and Validating Inhibition of N-Alkyl-5-hydroxypyrimidinone Carboxamides against Mtb in Vitro and ex Vivo. In vitro efficacy was performed in aerobic and anaerobic conditions. For aerobic conditions, logarithmically growing *Mtb* (OD_{650} 0.2) was diluted 1000-fold in 1 mL of 7H9/ADC media and exposed to 1×, 5×, 10×, 20×, and 50× MIC of **P01** for up to 7 days in duplicates. After 1, 2, 4, and 7 days of treatment, appropriate cell dilutions were plated on 7H11/OADC plates for CFU enumeration. For anaerobic conditions, *Mtb* was cultured in the self-generated oxygen-depletion model as previously described.[46] One milliliter of anaerobic *Mtb* culture was exposed to 1×, 5×, 10×, 20×, and 50× MIC of **P01** in an anaerobic chamber for 7 days. Diluted cells were plated on 7H11/OADC plates for CFU enumeration.

For the ex vivo efficacy test, J774 cells (5×10^5 cells/well) were seeded in flat-bottom 24-well plates (Corning Inc.) in DMEM GlutaMAX (Gibco/ThermoFisher Scientific) supplemented with 10% fetal-bovine serum, 20 mM HEPES, and 0.5 mM sodium pyruvate (hereafter abbreviated as DMEM/FBS). Cells were infected with *Mtb* (5×10^5 cells/well, MOI 1) for 24 h; this was followed by medium removal and washing (2×) with an equal volume of Dulbecco's PBS. Infected cells were fed DMEM/FBS and exposed to test compounds at 1×, 10×, 20×, and 50× MIC in medium (500 μL/well). Cells were incubated at 37 °C with 95% humidity and 5% CO_2 in an incubator for 7 days. The medium was changed every 4 days. After 4 and 7 days of incubation, 0.1% SDS was added to each well to lyse the J774 cells. After 5 min, the lysate was thoroughly mixed and diluted in 7H9/ADC, and appropriate dilutions were plated in duplicate on 7H11/OADC plates.

Generation and Characterization of N-Alkyl-5-hydroxypyrimidinone Carboxamide Resistant Mutants. To generate mutants against the *N*-alkyl-5-hydroxypyrimidinone carboxamide scaffold, 10^7, 10^8, and 10^9 cells of *Mtb* H37Rv were plated on 7H11/OADC plates containing with 2×, 5×, and 10× MIC of **P01** with drug-free plates used to enumerate bacterial load. The plates were incubated at 37 °C for 4 weeks. After 4 weeks, 24 colonies on 10× MIC of **P01** were picked and inoculated in 7H9/ADC medium and MIC-tested to confirm their resistance against **P01**. Genomic DNA of four mutants was isolated by the CTAB method.[47] Whole-genome sequencing was performed and analyzed as described.[48]

Generation and Testing of a Regulated Mutant of the dprE1−dprE2 Operon. *DprE12*−TetON1 was constructed using experimental strategies originally developed for the construction of dual-control mutants.[49] Briefly, *Mtb* H37Rv was transformed with a plasmid that integrated into the attachment site of phage L5 (*attL5*) and constitutively expressed *dprE1*, *dprE2*, *aftA*, and *embC*. This allowed deletion of the native copies of *dprE1*, *dprE2*, *aftA*, and *embC* by homologous recombination. The genotype of the resulting strain was verified by Southern blotting. We then replaced the constitutive-*dprE1−dprE2−aftA−embC*-expression plasmid with one in which transcription of *dprE1* and *dprE2* was susceptible to repression by the tetracycline repressor (TetR). In the resulting strain, *dprE12*−TetON1, expression of *aftA* and *embC* remained constitutive, but transcription of *dprE1* and *dprE2* could be increased with anhydrotetracycline. The *dprE12*−TetON1 mutant was maintained in 7H9-based growth medium supplemented with 500 ng/mL anhydrotetracycline/25 μg/mL kanamycin/50 μg/mL hygromycin. To assess the on-target effects of the compounds, cells were harvested, washed, and diluted in drug-free 7H9-based medium to an OD_{580nm} of 0.01. The cell suspension was split in two, and anhydrotetracycline was added (500 ng/mL) to one of the cultures. Cell suspensions (49.5 μL/well) were transferred to 384-well, black, clear-bottom plates containing a 14-point 2-fold drug dilution in DMSO, giving a final DMSO concentration of 1%. Positive-control drugs included the benzothiazinone BTZ043 and TCA1, and the negative-control drugs, which show no shift in susceptibility upon transcriptional repression, included ciprofloxacin (data not shown), ethambutol, linezolid (data

DOI: 10.1021/acs.jmedchem.8b00883
J. Med. Chem. 2018, 61, 9952−9965

not shown), and isoniazid (data not shown). Plates were wrapped in aluminum foil in stacks of three and incubated at 37 °C with 5% CO_2, and the OD_{580nm} was recorded at day 10.

*Pharmacokinetic Study of **P01**.* Animal studies were carried out in accordance with the Guide for the Care and Use of Laboratory Animals of the National Institutes of Health with approval from the Committee on the Ethics of Animal Experiments of the National Institute of Allergy and Infectious Diseases (LCID-4). Female mice (5 weeks of age) were purchased from Taconic Biosciences and allowed to acclimatize for at least 1 week prior to handling. The **P01** suspension was mixed with 1% carboxy methyl cellulose in a mortar and pestle, transferred to a vial, probe-sonicated until homogeneous in appearance, and then stirred overnight. Fifteen mice were administered 10 mg/kg **P01** in 0.2 mL by gavage, and 0.1 mL of blood was collected twice from each animal over the experiment and centrifuged to prepare serum.

Serum samples (five per time point: 0.5, 1, 2, 4, 6, and 24 h) for **P01** were prepared by mixing 50 μL aliquots of sample, 20 μL of aqueous 1% formic acid, and 50 μL of a cocktail of internal standards (various *Mtb* active compounds) followed by 400 μL of an acetonitrile/MeOH mixture (3:1) to precipitate proteins. The sample was centrifuged at 9450*g* for 5 min, and the supernatant was removed for tandem-mass-spectrometry analysis. The calibration curve was based on the internal standard with the best correlation coefficient and fit. Pharmacokinetic parameters were calculated using PK Solutions 2.0 (Summit Research Services).

Drug quantitation was performed by LC-MS/MS using an Agilent 1290 Infinity HPLC coupled to an Agilent 6460C triple-quadrupole tandem-mass-selective detector (QqQ). Water was supplied from a Barnstead nanopure Diamond system with a minimum resistivity of 18.1 MΩ·cm, and HPLC-grade acetonitrile and 98% formic acid were from EMD Millipore Corporation. Mobile phase A consisted of nanopure water, and mobile phase B consisted of acetonitrile, and each was spiked with 0.1% (v/v) formic acid. Each sample (5 μL) was injected into a 2.1 × 50 mm Agilent EclipsePlus C_{18} 1.7 μm 100 Å column. The HPLC was supplied mobile phase at 0.8 mL/min with a starting gradient of 8% acetonitrile, which was held for 15 s; this was followed by a linear gradient to 95% acetonitrile in 5.25 min, which was then held for 2 min. The QqQ detection was performed in MRM mode with positive-mode electrospray ionization. The tandem MRM signal was produced by converting the M + H^+ precursor ion for **P01** into the product ion *m*/*z* 91.1 with a collision energy (CE) of 28 V.

Molecular Modeling. The *Mtb* DprE1 crystal structure in the public domain was retrieved from PDB (PDB code: 4P8N).[50] This crystal structure had a noncovalently bound ligand[51] and two chains in an asymmetric unit with a high resolution of 1.79 Å. Chain A of this structure was selected for the docking study. The Schrödinger modeling package[52] was used to prepare the protein structure and to generate the Grid file for docking studies. The protein-preparation process involved the following steps: assigning bond orders to protein and ligand molecules, adding hydrogen atoms, creating disulfide bonds, sampling water orientations, assigning protein and ligand charge states at pH 7.0, and minimizing all hydrogen atoms while fixing the positions of all protein heavy atoms. The docking grid was generated using a box of dimensions 20 × 20 × 20 Å around the crystal ligand. The ligand docking was carried with the Glide method.[53] **P01** was docked into the DprE1 binding site using both the SP and XP sampling methods in Glide. The best model was selected via visual inspection with the SAR information in mind.

■ ASSOCIATED CONTENT

Supporting Information

The Supporting Information is available free of charge on the ACS Publications website at DOI: 10.1021/acs.jmedchem.8b00883.

Characterization data of **P01**−**P18** including ^1H, ^{13}C, and HRMS spectra and purities (PDF)

Molecular-formula strings (CSV)

Molecular modeling of **P01** (PDB)

■ AUTHOR INFORMATION

Corresponding Author

*Tel.: +1-301-435-7509. Fax: +1-301-480-3506. E-mail: cbarry@niaid.nih.gov.

ORCID

Sangmi Oh: 0000-0003-0895-1110

Helena I. M. Boshoff: 0000-0002-4333-206X

Clifton E. Barry, III: 0000-0002-2927-270X

Notes

The authors declare no competing financial interest.

■ ACKNOWLEDGMENTS

We specially thank Dr. Thomas R. Webb, Dr. Vincent A. Boyd, Jeanine Price, and Parimala Hanumesh of the Medicinal Chemistry Center at St. Jude Children's Research Hospital for their assistance in providing the small-molecule library. This study was funded in part by the intramural research program of the NIAID, NIH, and in part by grants to C.E.B. and the FNIH and to D.S. by the Bill and Melinda Gates Foundation (OPP1024021 and OPP1024065).

■ ABBREVIATIONS USED

DprE1, decaprenylphosphoryl-β-D-ribose 2′-oxidase; *Mtb*, *Mycobacterium tuberculosis*; TB, tuberculosis; WHO, World Health Organization; SAR, structure−activity relationship; MIC, minimum inhibitory concentration; DPR, decaprenylphosphoryl ribose; DPA, decaprenylphosphoryl arabinose; NMR, nuclear magnetic resonance; LRMS, low-resolution mass spectrometry; HRMS, high-resolution mass spectrometry; LC-MS, liquid chromatography−mass spectrometry; ESI, electrospray ionization; TLC, thin-layer chromatography

■ REFERENCES

(1) *Global Tuberculosis Report 2017*; World Health Organization: Geneva, 2017.

(2) Tiberi, S.; Muñoz-Torrico, M.; Duarte, R.; Dalcolmo, M.; D'Ambrosio, L.; Migliori, G.-B. New drugs and perspectives for new anti-tuberculosis regimens. *Pulmonology* **2018**, *24*, 86−98.

(3) Vjecha, M. J.; Tiberi, S.; Zumla, A. Accelerating the development of therapeutic strategies for drug-resistant tuberculosis. *Nat. Rev. Drug Discovery* **2018**, *17*, 607.

(4) Smith, R. L.; Maguire, M. E. Microbial magnesium transport: unusual transporters searching for identity. *Mol. Microbiol.* **1998**, *28*, 217−226.

(5) Draper, D. E.; Grilley, D.; Soto, A. M. Ions and RNA folding. *Annu. Rev. Biophys. Biomol. Struct.* **2005**, *34*, 221−243.

(6) Guo, L.; Lim, K. B.; Poduje, C. M.; Daniel, M.; Gunn, J. S.; Hackett, M.; Miller, S. I. Lipid A acylation and bacterial resistance against vertebrate antimicrobial peptides. *Cell* **1998**, *95*, 189−198.

(7) Perez, J. C.; Shin, D.; Zwir, I.; Latifi, T.; Hadley, T. J.; Groisman, E. A. Evolution of a bacterial regulon controlling virulence and Mg^{2+} homeostasis. *PLoS Genet.* **2009**, *5*, e1000428.

(8) Asensio, J. G.; Maia, C.; Ferrer, N. L.; Barilone, N.; Laval, F.; Soto, C. Y.; Winter, N.; Daffé, M.; Gicquel, B.; Martín, C.; Jackson, M. The virulence-associated two-component PhoP-PhoR system controls the biosynthesis of polyketide-derived lipids in *Mycobacterium tuberculosis*. *J. Biol. Chem.* **2006**, *281*, 1313−1316.

(9) Walters, S. B.; Dubnau, E.; Kolesnikova, I.; Laval, F.; Daffé, M.; Smith, I. The *Mycobacterium tuberculosis* PhoPR two-component system regulates genes essential for virulence and complex lipid biosynthesis. *Mol. Microbiol.* **2006**, *60*, 312−330.

DOI: 10.1021/acs.jmedchem.8b00883
J. Med. Chem. 2018, 61, 9952−9965

(10) Lee, E.-J.; Pontes, M. H.; Groisman, E. A. A bacterial virulence protein promotes pathogenicity by inhibiting the bacterium's own F1Fo ATP synthase. *Cell* **2013**, *154*, 146−156.
(11) Buchmeier, N.; Blanc-Potard, A.; Ehrt, S.; Piddington, D.; Riley, L.; Groisman, E. A. A parallel intraphagosomal survival strategy shared by *Mycobacterium tuberculosis* and *Salmonella enterica*. *Mol. Microbiol.* **2000**, *35*, 1375−1382.
(12) Goodsmith, N.; Guo, X. V.; Vandal, O. H.; Vaubourgeix, J.; Wang, R.; Botella, H.; Song, S.; Bhatt, K.; Liba, A.; Salgame, P.; Schnappinger, D.; Ehrt, S. Disruption of an *M. tuberculosis* membrane protein causes a magnesium-dependent cell division defect and failure to persist in mice. *PLoS Pathog.* **2015**, *11*, e1004645.
(13) Lechartier, B.; Rybniker, J.; Zumla, A.; Cole, S. T. Tuberculosis drug discovery in the post-post-genomic era. *EMBO Mol. Med.* **2014**, e201201772.
(14) Welsch, M. E.; Snyder, S. A.; Stockwell, B. R. Privileged scaffolds for library design and drug discovery. *Curr. Opin. Chem. Biol.* **2010**, *14*, 347−361.
(15) DeSimone, R. W.; Currie, K. S.; Mitchell, S. A.; Darrow, J. W.; Pippin, D. A. Privileged structures: applications in drug discovery. *Comb. Chem. High Throughput Screening* **2004**, *7*, 473−493.
(16) Duarte, C. D.; Barreiro, E. J.; Fraga, C. A. M. Privileged structures: a useful concept for the rational design of new lead drug candidates. *Mini-Rev. Med. Chem.* **2007**, *7*, 1108−1119.
(17) Summa, V.; Petrocchi, A.; Matassa, V. G.; Taliani, M.; Laufer, R.; De Francesco, R.; Altamura, S.; Pace, P. HCV NS5b RNA-dependent RNA polymerase inhibitors: from α,γ-diketoacids to 4,5-dihydroxypyrimidine- or 3-methyl-5-hydroxypyrimidinonecarboxylic acids. Design and synthesis. *J. Med. Chem.* **2004**, *47*, 5336−5339.
(18) Petrocchi, A.; Koch, U.; Matassa, V. G.; Pacini, B.; Stillmock, K. A.; Summa, V. From dihydroxypyrimidine carboxylic acids to carboxamide HIV-1 integrase inhibitors: SAR around the amide moiety. *Bioorg. Med. Chem. Lett.* **2007**, *17*, 350−353.
(19) Hu, Y.-G.; Li, L.; Zhang, Q.-Y.; Zhang, A.-N.; Feng, C.; He, P. Efficient synthesis and fungicidal activities of strobilurin analogues containing benzofuro [3,2-d]-1,2,4-triazolo[1,5-a]pyrimidinone side chains. *Heterocycl. Commun.* **2015**, *21*, 345−348.
(20) Sayed, H. H.; Abbas, H.-A. S.; Morsi, E. M. H.; Amr, A. E.-G. E.; Abdelwahad, N. A. M. Antimicrobial activity of some synthesized glucopyranosyl-pyrimidine carbonitrile and fused pyrimidine systems. *Acta Pharm.* **2010**, *60*, 479−491.
(21) Parameshwarappa, G.; Sangapure, S. S. Synthesis and antimicrobial activities of 2-aryl-3,4-dihydro-4-oxo-5-bromobenzofuro[3,2-*d*]pyrimidines. *Org. Chem. Ind. J.* **2009**, *5*, 80−82.
(22) Sasi, N. K.; Tiwari, K.; Soon, F.-F.; Bonte, D.; Wang, T.; Melcher, K.; Xu, H. E.; Weinreich, M. The potent Cdc7-Dbf4 (DDK) kinase inhibitor XL413 has limited activity in many cancer cell lines and discovery of potential new DDK inhibitor scaffolds. *PLoS One* **2014**, *9*, e113300.
(23) Evering, T. H.; Markowitz, M. Raltegravir: an integrase inhibitor for HIV-1. *Expert Opin. Invest. Drugs* **2008**, *17*, 413−422.
(24) Mouscadet, J.-F.; Tchertanov, L. Raltegravir: molecular basis of its mechanism of action. *Eur. J. Med.Res.* **2009**, *14*, 5−16.
(25) Summa, V.; Petrocchi, A.; Bonelli, F.; Crescenzi, B.; Donghi, M.; Ferrara, M.; Fiore, F.; Gardelli, C.; Gonzalez Paz, O.; Hazuda, D. J.; Jones, P.; Kinzel, O.; Laufer, R.; Monteagudo, E.; Muraglia, E.; Nizi, E.; Orvieto, F.; Pace, P.; Pescatore, G.; Scarpelli, R.; Stillmock, K.; Witmer, M. V.; Rowley, M. Discovery of raltegravir, a potent, selective orally bioavailable HIV-integrase inhibitor for the treatment of HIV-AIDS infection. *J. Med. Chem.* **2008**, *51*, 5843−5855.
(26) Boyd, V. A.; Mason, J.; Hanumesh, P.; Price, J.; Russell, C. J.; Webb, T. R. 2-Substituted-4,5-dihydroxypyrimidine-6-carboxamide antiviral targeted libraries. *J. Comb. Chem.* **2009**, *11*, 1100−1104.
(27) Naran, K.; Moosa, A.; Barry, C. E., 3rd; Boshoff, H. I.; Mizrahi, V.; Warner, D. F. Bioluminescent reporters for rapid mechanism of action assessment in tuberculosis drug discovery. *Antimicrob. Agents Chemother.* **2016**, *60*, 6748−6757.
(28) Arora, K.; Ochoa-Montaño, B.; Tsang, P. S.; Blundell, T. L.; Dawes, S. S.; Mizrahi, V.; Bayliss, T.; Mackenzie, C. J.; Cleghorn, L. A. T.; Ray, P. C.; Wyatt, P. G.; Uh, E.; Lee, J.; Barry, C. E., 3rd; Boshoff, H. I. Respiratory flexibility in response to inhibition of cytochrome C oxidase in *Mycobacterium tuberculosis*. *Antimicrob. Agents Chemother.* **2014**, *58*, 6962−6965.
(29) Pace, P.; Di Francesco, M. E.; Gardelli, C.; Harper, S.; Muraglia, E.; Nizi, E.; Orvieto, F.; Petrocchi, A.; Poma, M.; Rowley, M.; Scarpelli, R.; Laufer, R.; Gonzalez Paz, O.; Monteagudo, E.; Bonelli, F.; Hazuda, D.; Stillmock, K. A.; Summa, V. Dihydroxypyrimidine-4-carboxamides as novel potent and selective HIV integrase inhibitors. *J. Med. Chem.* **2007**, *50*, 2225−2239.
(30) Tang, J.; Maddali, K.; Pommier, Y.; Sham, Y. Y.; Wang, Z. Scaffold rearrangement of dihydroxypyrimidine inhibitors of HIV integrase: Docking model revisited. *Bioorg. Med. Chem. Lett.* **2010**, *20*, 3275−3279.
(31) Wang, Z.; Wang, M.; Yao, X.; Li, Y.; Qiao, W.; Geng, Y.; Liu, Y.; Wang, Q. Hydroxyl may not be indispensable for raltegravir: Design, synthesis and SAR studies of raltegravir derivatives as HIV-1 inhibitors. *Eur. J. Med. Chem.* **2012**, *50*, 361−369.
(32) Wang, Y.; Rong, J.; Zhang, B.; Hu, L.; Wang, X.; Zeng, C. Design and synthesis of *N*-methylpyrimidone derivatives as HIV-1 integrase inhibitors. *Bioorg. Med. Chem.* **2015**, *23*, 735−741.
(33) Gembus, V.; Furman, C.; Millet, R.; Mansouri, R.; Chavatte, P.; Levacher, V.; Brière, J.-F. Scaffold hopping strategy toward original pyrazolines as selective CB2 receptor ligands. *Eur. J. Med. Chem.* **2012**, *58*, 396−404.
(34) Wayne, L. G.; Hayes, L. G. An *in vitro* model for sequential study of shiftdown of *Mycobacterium tuberculosis* through two stages of nonreplicating persistence. *Infect. Immun.* **1996**, *64*, 2062−2069.
(35) Mikušová, K.; Huang, H.; Yagi, T.; Holsters, M.; Vereecke, D.; D'Haeze, W.; Scherman, M. S.; Brennan, P. J.; McNeil, M. R.; Crick, D. C. Decaprenylphosphoryl arabinofuranose, the donor of the D-arabinofuranosyl residues of mycobacterial arabinan, is formed via a two-step epimerization of decaprenylphosphoryl ribose. *J. Bacteriol.* **2005**, *187*, 8020−8025.
(36) Riccardi, G.; Pasca, M. R.; Chiarelli, L. R.; Manina, G.; Mattevi, A.; Binda, C. The DprE1 enzyme, one of the most vulnerable targets of *Mycobacterium tuberculosis*. *Appl. Microbiol. Biotechnol.* **2013**, *97*, 8841−8848.
(37) Chikhale, R. V.; Barmade, M. A.; Murumkar, P. R.; Yadav, M. R. An Overview of the development of DprE1 Inhibitors for combating the menace of tuberculosis. *J. Med. Chem.* **2018**, *61*, 8563.
(38) *Phase 2a Study of PBTZ169*; NCT03334734; ClinicalTrials.gov, 2018. Available at https://clinicaltrials.gov/ct2/show/study/NCT03334734.
(39) Wang, F.; Sambandan, D.; Halder, R.; Wang, J.; Batt, S. M.; Weinrick, B.; Ahmad, I.; Yang, P.; Zhang, Y.; Kim, J.; Hassani, M.; Huszar, S.; Trefzer, C.; Ma, Z.; Kaneko, T.; Mdluli, K. E.; Franzblau, S.; Chatterjee, A. K.; Johnsson, K.; Mikusova, K.; Besra, G. S.; Fütterer, K.; Robbins, S. H.; Barnes, S. W.; Walker, J. R.; Jacobs, W. R., Jr.; Schultz, P. G. Identification of a small molecule with activity against drug-resistant and persistent tuberculosis. *Proc. Natl. Acad. Sci. U. S. A.* **2013**, *110*, E2510−E2517.
(40) Warrier, T.; Kapilashrami, K.; Argyrou, A.; Ioerger, T. R.; Little, D.; Murphy, K. C.; Nandakumar, M.; Park, S.; Gold, B.; Mi, J.; Zhang, T.; Meiler, E.; Rees, M.; Somersan-Karakaya, S.; Porras-De Francisco, E.; Martinez-Hoyos, M.; Burns-Huang, K.; Roberts, J.; Ling, Y.; Rhee, K. Y.; Mendoza-Losana, A.; Luo, M.; Nathan, C. F. *N*-methylation of a bactericidal compound as a resistance mechanism in *Mycobacterium tuberculosis*. *Proc. Natl. Acad. Sci. U. S. A.* **2016**, *113*, E4523−E4530.
(41) Makarov, V.; Manina, G.; Mikusova, K.; Möllmann, U.; Ryabova, O.; Saint-Joanis, B.; Dhar, N.; Pasca, M. R.; Buroni, S.; Lucarelli, A. P.; Milano, A.; De Rossi, E.; Belanova, M.; Bobovska, A.; Dianiskova, P.; Kordulakova, J.; Sala, C.; Fullam, E.; Schneider, P.; McKinney, J. D.; Brodin, P.; Christophe, T.; Waddell, S.; Butcher, P.; Albrethsen, J.; Rosenkrands, I.; Brosch, R.; Nandi, V.; Bharath, S.; Gaonkar, S.; Shandil, R. K.; Balasubramanian, V.; Balganesh, T.; Tyagi, S.; Grosset, J.; Riccardi, G.; Cole, S. T. Benzothiazinones kill

DOI: 10.1021/acs.jmedchem.8b00883
J. Med. Chem. 2018, 61, 9952−9965

Mycobacterium tuberculosis by blocking arabinan synthesis. *Science* **2009**, *324*, 801−804.
(42) *ACD/Labs PhysChem Suite V 11.0*; Advanced Chemistry Development Inc.: Toronto, Canada, 2007.
(43) Campaniço, A.; Moreira, R.; Lopes, F. Drug discovery in tuberculosis. New drug targets and antimycobacterial agents. *Eur. J. Med. Chem.* **2018**, *150*, 525−545.
(44) De Voss, J. J.; Rutter, K.; Schroeder, B. G.; Su, H.; Zhu, Y.; Barry, C. E., 3rd. The salicylate-derived mycobactin siderophores of *Mycobacterium tuberculosis* are essential for growth in macrophages. *Proc. Natl. Acad. Sci. U. S. A.* **2000**, *97*, 1252−1257.
(45) Duckworth, B. P.; Wilson, D. J.; Nelson, K. M.; Boshoff, H. I.; Barry, C. E., 3rd; Aldrich, C. C. Development of a selective activity-based probe for adenylating enzymes: profiling MbtA involved in siderophore biosynthesis from *Mycobacterium tuberculosis*. *ACS Chem. Biol.* **2012**, *7*, 1653−1658.
(46) Boshoff, H. I. M.; Xu, X.; Tahlan, K.; Dowd, C. S.; Pethe, K.; Camacho, L. R.; Park, T.-H.; Yun, C.-S.; Schnappinger, D.; Ehrt, S.; Williams, K. J.; Barry, C. E., 3rd. Biosynthesis and recycling of nicotinamide cofactors in *Mycobacterium tuberculosis* an essential role for NAD in nonreplicating bacilli. *J. Biol. Chem.* **2008**, *283*, 19329−19341.
(47) Park, Y.; Pacitto, A.; Bayliss, T.; Cleghorn, L. A. T.; Wang, Z.; Hartman, T.; Arora, K.; Ioerger, T. R.; Sacchettini, J.; Rizzi, M.; Donini, S.; Blundell, T. L.; Ascher, D. B.; Rhee, K.; Breda, A.; Zhou, N.; Dartois, V.; Jonnala, S. R.; Via, L. E.; Mizrahi, V.; Epemolu, O.; Stojanovski, L.; Simeons, F.; Osuna-Cabello, M.; Ellis, L.; MacKenzie, C. J.; Smith, A. R. C.; Susan, H.; Davis, S. H.; Murugesan, D.; Buchanan, K. I.; Turner, P. A.; Huggett, M.; Zuccotto, F.; Rebollo-Lopez, M. J.; Lafuente-Monasterio, M. J.; Sanz, O.; Diaz, G. S.; Lelièvre, J.; Ballell, L.; Selenski, C.; Axtman, M.; Ghidelli-Disse, S.; Pflaumer, H.; Bösche, M.; Drewes, G.; Freiberg, G. M.; Kurnick, M. D.; Srikumaran, M.; Kempf, D. J.; Green, S. R.; Ray, P. C.; Read, K.; Wyatt, P.; Barry, C. E., 3rd; Boshoff, H. I. Essential but not vulnerable: indazole sulfonamides targeting inosine monophosphate dehydrogenase as potential leads against *Mycobacterium tuberculosis*. *ACS Infect. Dis.* **2017**, *3*, 18−33.
(48) Ioerger, T. R.; Feng, Y.; Ganesula, K.; Chen, X.; Dobos, K. M.; Fortune, S.; Jacobs, W. R., Jr.; Mizrahi, V.; Parish, T.; Rubin, E.; Sassetti, C.; Sacchettini, J. C. Variation among genome sequences of H37Rv strains of *Mycobacterium tuberculosis* from multiple laboratories. *J. Bacteriol.* **2010**, *192*, 3645−3653.
(49) Schnappinger, D.; O'Brien, K. M.; Ehrt, S. Construction of conditional knockdown mutants in mycobacteria. *Methods Mol. Biol.* **2015**, *1285*, 151−175.
(50) Berman, H.; Westbrook, J.; Feng, Z.; Gilliland, G.; Bhat, T. N.; Weissig, H.; Shindyalov, I. N.; Bourne, P. E. The protein data bank. *Nucleic Acids Res.* **2000**, *28*, 235−242.
(51) Neres, J.; Hartkoorn, R. C.; Chiarelli, L. R.; Gadupudi, R.; Pasca, M. R.; Mori, G.; Venturelli, A.; Savina, S.; Makarov, V.; Kolly, G. S.; Molteni, E.; Binda, C.; Dhar, N.; Ferrari, S.; Brodin, P.; Delorme, V.; Landry, V.; de Jesus Lopes Ribeiro, A. L.; Farina, D.; Saxena, P.; Pojer, F.; Carta, A.; Luciani, R.; Porta, A.; Zanoni, G.; De Rossi, E.; Costi, M. P.; Riccardi, G.; Cole, S. T. 2-Carboxyquinoxalines kill *Mycobacterium tuberculosis* through noncovalent inhibition of DprE1. *ACS Chem. Biol.* **2015**, *10*, 705−714.
(52) *Schrödinger Release 2017-1: Drug Discovery Suite*; Schrödinger, LLC: New York, 2017.
(53) Friesner, R. A.; Banks, J. L.; Murphy, R. B.; Halgren, T. A.; Klicic, J. J.; Mainz, D. T.; Repasky, M. P.; Knoll, E. H.; Shelley, M.; Perry, J. K.; Shaw, D. E.; Francis, P.; Shenkin, P. S. Glide: a new approach for rapid, accurate docking and scoring. 1. Method and assessment of docking accuracy. *J. Med. Chem.* **2004**, *47*, 1739−1749.

DOI: 10.1021/acs.jmedchem.8b00883
J. Med. Chem. 2018, 61, 9952−9965